

# A CCaMK/Cyclops response element in the promoter of *Lotus japonicus* calcium-binding protein 1 (CBP1) mediates transcriptional activation in root symbioses

Xiaoyun Gong<sup>1</sup> , Elaine Jensen<sup>2,3</sup> , Simone Bucerius<sup>1</sup>  and Martin Parniske<sup>1,2</sup> 

<sup>1</sup>Genetics, Faculty of Biology, LMU Munich, Grosshaderner Str. 2-4, D-82152 Martinsried, Germany; <sup>2</sup>The Sainsbury Laboratory, Colney Lane, Norwich, NR4 7UH, UK; <sup>3</sup>Institute of Biological, Environmental and Rural Sciences, Aberystwyth University, Aberystwyth, Wales, Ceredigion, SY23 3EB, UK

## Summary

Author for correspondence:  
Martin Parniske  
Email: [parniske@lmu.de](mailto:parniske@lmu.de)

Received: 13 August 2021  
Accepted: 24 December 2021

*New Phytologist* (2022) **235**: 1196–1211  
doi: 10.1111/nph.18112

**Key words:** arbuscular mycorrhizal (AM) symbiosis, DNA methylation, ethyl methanesulphonate (EMS) mutagenesis, epigenetic modification, nitrogen-fixing root nodule symbiosis, T-DNA insertion, tissue specificity, transcriptional regulation.

- Early gene expression in arbuscular mycorrhiza (AM) and the nitrogen-fixing root nodule symbiosis (RNS) is governed by a shared regulatory complex. Yet many symbiosis-induced genes are specifically activated in only one of the two symbioses.
- The *Lotus japonicus* T-DNA insertion line T90, carrying a promoterless *uidA* (*GUS*) gene in the promoter of *Calcium Binding Protein 1* (*CBP1*) is exceptional as it exhibits *GUS* activity in both root endosymbioses. To identify the responsible *cis*- and *trans*-acting factors, we subjected deletion/modification series of *CBP1* promoter: reporter fusions to transactivation and spatio-temporal expression analysis and screened ethyl methanesulphonate (EMS)-mutagenized T90 populations for aberrant *GUS* expression.
- We identified one *cis*-regulatory element required for *GUS* expression in the epidermis and a second element, necessary and sufficient for transactivation by the calcium and calmodulin-dependent protein kinase (CCaMK) in combination with the transcription factor Cyclops and conferring gene expression during both AM and RNS. Lack of *GUS* expression in T90 *white* mutants could be traced to DNA hypermethylation detected in and around this element.
- We concluded that the CCaMK/Cyclops complex can contribute to at least three distinct gene expression patterns on its direct target promoters *NIN* (RNS), *RAM1* (AM), and *CBP1* (AM and RNS), calling for yet-to-be identified specificity-conferring factors.

## Introduction

As main constituents of nucleotides, proteins and nucleic acids, nitrogen and phosphate are essential for life (Bowler *et al.*, 2010). Two types of plant root endosymbiosis, the arbuscular mycorrhiza (AM) and the nitrogen-fixing root nodule symbiosis (RNS) hold promise for sustainable agriculture. AM and RNS greatly benefit plant nutrition by improving nutrient uptake from the soil and providing ammonium as a nitrogen source, respectively. Root nodule symbiosis can significantly reduce the demand for chemical nitrogen fertilizer application, hence reducing fossil fuel consumption and, once globally adjusted to a sustainable scale, the negative ecological impact imposed by the release of ammonium and nitrogen oxides into the atmosphere, groundwater, rivers, lakes and the sea (Fowler *et al.*, 2013).

Establishment of both AM and RNS requires chemical communications between symbiotic partners that induce concerted structural modification and rearrangement of the host cells, both controlled by a cohort of transcriptional circuitries. To unravel the genes underlying the development of these two important symbioses, transcriptome analysis has been employed and led to a catalogue of symbiosis-regulated genes that are responsive to AM

(Liu *et al.*, 2003; Kistner *et al.*, 2005; Hoge Kamp *et al.*, 2011; Gutjahr *et al.*, 2015) or RNS (Demina *et al.*, 2013; Breakspear *et al.*, 2014; Roux *et al.*, 2014). Although many symbiosis-regulated genes are expressed specifically in either RNS or AM, such as *Nodule Inception* (*NIN*) (Schäuser *et al.*, 1999; Kumar *et al.*, 2020) or *Reduced Arbuscular Mycorrhiza 1* (*RAM1*) (Gobbato *et al.*, 2012), respectively, a small subset of genes appears to be induced in both symbioses (varying between 2% to maximum 28% of differentially induced genes in either symbiosis in different studies; Manthey *et al.*, 2004; Hohnjec *et al.*, 2005; Deguchi *et al.*, 2007; Tromas *et al.*, 2012; Nanjareddy *et al.*, 2017; Sakamoto *et al.*, 2019). Genes with a common symbiotic expression profile include a symbiosis induced Subtilase (*SbtS*) (Kistner *et al.*, 2005; Takeda *et al.*, 2007, 2009), *Vesicle-Associated Membrane Protein 72* (Ivanov *et al.*, 2012), *ENOD11* (Boisson-Dernier *et al.*, 2005), *Vapyrin* (Murray *et al.*, 2011) and *ABC-B transporters in Mycorrhization and Nodulation* (Roy *et al.*, 2021).

The question how the three different patterns of gene expression in response to symbiotic bacteria and fungi are accomplished, is particularly puzzling, because early gene expression in both symbioses depends on the same subset of the so called

‘common symbiosis genes’, some of which encode proteins involved in early signal transduction processes (Kistner *et al.*, 2005; Oldroyd, 2013). A key to specificity may be at the initiation step of the signalling cascade because microsymbiont-derived molecules, lipo-chitoooligosaccharides (LCOs) with specificity-conferring decorations produced by nitrogen-fixing bacteria (collectively referred to as Nod factor), or LCOs and short-chain chitin oligosaccharides (COs) by AM fungi (Maillet *et al.*, 2011; Feng *et al.*, 2019) are believed to be perceived by distinct complexes comprising LysM type receptor-like kinases (Radutoiu *et al.*, 2003; Zhang *et al.*, 2021). Symbiosis receptor-like kinase (SymRK) (Endre *et al.*, 2002; Stracke *et al.*, 2002) can associate with specific LysM receptors and thus forms a conceptual link between the perception of microbial (L)COs and the initiation of symbiotic downstream responses (Antolín-Llovera *et al.*, 2014; Ried *et al.*, 2014). A hallmark of the common signalling process is the generation of nuclear calcium oscillation (or spiking) (Sieberer *et al.*, 2009) facilitated by ion channels and transporters on the nuclear envelope (see review by Kim *et al.*, 2019). Calcium spiking is postulated to act as a second messenger which is presumably decoded in the nucleus by a calcium-calmodulin dependent kinase (CCaMK) (Lévy *et al.*, 2004; Tirichine *et al.*, 2006). CCaMK is activated via binding of a, yet to be identified, calmodulin, and interacts with and phosphorylates Cyclops, a DNA-binding transcription factor (Yano *et al.*, 2008; Miller *et al.*, 2013; Singh *et al.*, 2014). This protein complex is required for both RNS and AM to activate symbiosis-related genes, e.g. *RAM1* during AM (Pimprikar *et al.*, 2016); or *NIN* and *ERF* required for nodulation 1 (*ERN1*) during RNS (Singh *et al.*, 2014; Cerri *et al.*, 2017).

*Cis*-acting regulatory sequences (*cis*-elements) are crucial for temporal and/or spatial regulation of gene expression in eukaryotes. In agreement with this, RNS or AM-related *cis*-elements have been identified in the promoters or intronic regions of symbiosis-regulated genes (Pimprikar & Gutjahr, 2018; Liu *et al.*, 2019; Akamatsu *et al.*, 2020). Taking into account the three principally different expression patterns (AM-induced, RNS-induced and commonly induced) in the light of the postulate of a common symbiosis signalling pathway, it was hypothesized that the different gene expression patterns are achieved by two independent and symbiosis-specific pathways that act in parallel to the common signalling pathway (Schultze & Kondorosi, 1998). According to this model, dual gene expression in both symbioses could be achieved by promoters harbouring both AM-specific and RNS-specific *cis*-elements, thus accumulating the output of the two specific and independent pathways, or *cis*-elements exclusively responsive to the output of the common symbiosis pathway, or a mix of all three types of *cis*-elements.

To obtain further insights into the mechanisms that confer common symbiosis-related gene expression, we employed the *Lotus japonicus* promoter tagging line T90 (Webb *et al.*, 2000), which has served as a useful marker line for the study of plant symbiotic signal transduction over the last two decades (Kistner *et al.*, 2005; Gossmann *et al.*, 2012; Ried *et al.*, 2014; Banhara *et al.*, 2015). T90 carries a single copy of a T-DNA, containing a promoterless *GUS* gene, which is inserted in the promoter region

of the *calcium binding protein 1* (*CBP1*) gene (Fig. 1a). The T90 *GUS* gene expression was so far exclusively observed in plant roots inoculated with AM fungi (Kistner *et al.*, 2005) or rhizobia, including *Mesorhizobium loti* strain R7A in an NF-dependent manner (Webb *et al.*, 2000) and treated with *M. loti* strain R7A Nod factor (Webb *et al.*, 2000; Gossmann *et al.*, 2012) but in no other tissues or treatments tested (Kistner *et al.*, 2005; Gossmann *et al.*, 2012). For example, T90 *GUS* expression was neither

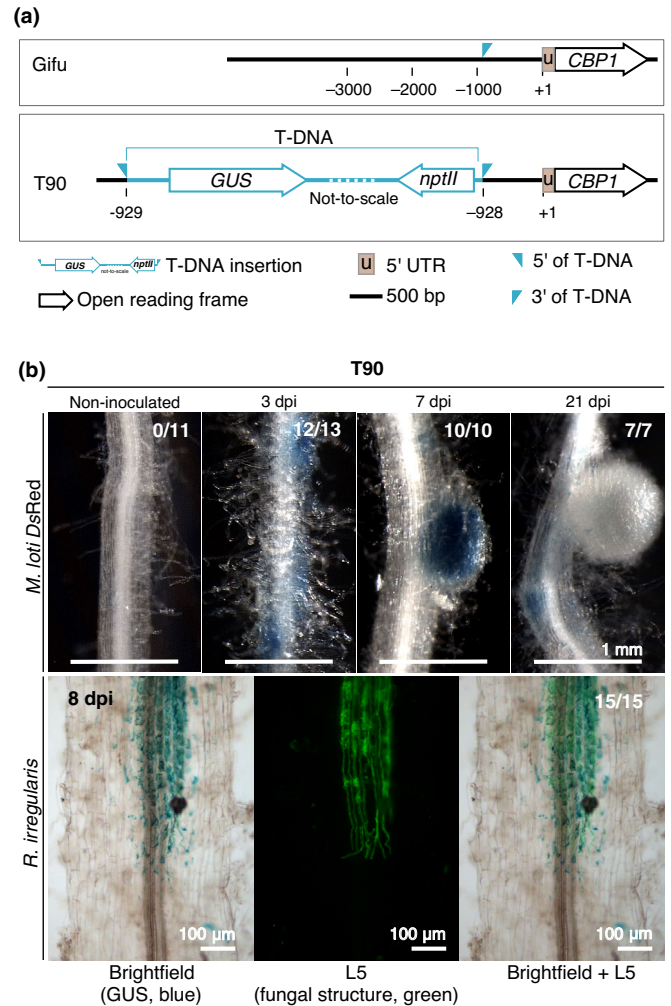


**Fig. 1** *GUS* expression pattern in T90 roots. (a) Position of the T-DNA insertion within the promoter of *CBP1* gene in the transgenic line T90. The respective region in *Lotus japonicus* ecotype Gifu is shown as a reference. (b) T90 roots were stained with 5-bromo-4-chloro-3-indolyl- $\beta$ -D-glucuronic acid (X-Gluc) to reveal a blue coloration generated by *GUS* enzyme activity at indicated days post-inoculation (dpi) with *Mesorhizobium loti* expressing *Discosoma* sp. red fluorescent protein (*M. loti* DsRed) or arbuscular mycorrhiza (AM) fungus *Rhizophagus irregularis*. Note the blue staining at 3 dpi in patches, the presence and absence of blue staining in the central nodule tissue at 7 dpi and 21 dpi, respectively. At 21 dpi, blue staining could be seen in the inner tissue of developing nodules, in contrast to mature nodules that remained white. Green, Alexa Fluor-488 WGA-stained *R. irregularis* visualized with a Leica Filter Cube L5 next to a brightfield image of the same root segment. #/# in (b), number of root system displaying *GUS* activity/total number of plants analysed. Bars, 1 mm unless stated otherwise. Sections of nodules or roots are displayed in Supporting Information Fig. S1.

detected in T90 shoots or leaves nor inducible by synthetic hormones 1-naphthaleneacetic acid (NAA) or 6-benzylaminopurine (6-BAP) (Webb *et al.*, 2000; Tuck, 2006). It was also not induced upon inoculation with the growth-promoting fungus *Serendipita indica* (previously known as *Piriformospora indica*) (Banhara *et al.*, 2015).

*GUS* expression in T90 only represents a specific aspect of the broader expression domain of *CBPI*: Northern blots with a *CBPI* probe yielded a hybridization signal in nodulated roots of T90 although at a lower intensity than in wild-type roots (Webb *et al.*, 2000). The authors concluded that the T90 T-DNA insertion did not fully abolish *CBPI* expression and postulated the presence of additional *cis*-regulatory elements in the 928 bp region between the T-DNA insertion site and the *CBPI* transcriptional start site (Webb *et al.*, 2000; Tuck, 2006). In agreement with this hypothesis, we observed that *CBPI<sub>pro</sub>:GUS* exhibited indeed a much broader expression domain as *GUS* in the T90 line.

This work aimed to decipher the molecular secret behind the common, yet exclusive symbiosis-induced gene expression pattern of T90. To this end, we performed a classical 'forward genetics' approach in which we generated an ethyl methanesulphonate (EMS)-mutagenized T90 population and screened M2 and M3 families for the loss and gain of *GUS* expression. In parallel, we analysed promoter deletion series of the *CBPI* and the T90 promoters to identify regions with relevance for symbiotic responsiveness.

## Materials and Methods

### Plant, bacterial and fungal material

*Lotus japonicus* genotypes used were Gifu (wild-type, accession B-129, Handberg & Stougaard, 1992); T90 (Webb *et al.*, 2000) and the EMS mutant derivatives of T90: T90 *white1* (original seeds harvested from plant L8668); T90 *white2* (original seeds harvested from plant L8686), T90 *white3* (original seeds harvested from plant L8687). Seed bag numbers are listed in Supporting Information Table S1.

*Mesorhizobium loti* MAFF 303099 constitutively expressing *Discosoma* sp. red fluorescent protein (*M. loti* DsRed) were used to inoculate *L. japonicus* roots. *M. loti* DsRed was grown in tryptone yeast (TY) extract liquid medium (Beringer, 1974) supplied with gentamicin (25 µg ml<sup>-1</sup>) shaken at 180 rounds per minute at 28°C and harvested by centrifugation at 3400 g for 10 min at room temperature (RT). *M. loti* DsRed was washed twice with FAB medium (500 µM MgSO<sub>4</sub>·7H<sub>2</sub>O; 250 µM KH<sub>2</sub>PO<sub>4</sub>; 250 µM KCl; 250 µM CaCl<sub>2</sub>·2H<sub>2</sub>O; 100 µM KNO<sub>3</sub>; 25 µM Fe-EDDHA, catalog no. F0527.0250, Duchefa Biochemie, Haarlem, the Netherlands; 50 µM H<sub>3</sub>BO<sub>3</sub>; 25 µM MnSO<sub>4</sub>·H<sub>2</sub>O; 10 µM ZnSO<sub>4</sub>·7H<sub>2</sub>O; 0.5 µM Na<sub>2</sub>MoO<sub>4</sub>·2H<sub>2</sub>O; 0.2 µM CuSO<sub>4</sub>·5H<sub>2</sub>O; 0.2 µM CoCl<sub>2</sub>·6H<sub>2</sub>O; pH 5.7), and resuspended in FAB medium to reach a final optical density at 600 nm (OD<sub>600</sub>) of 0.01 for inoculation.

The AM fungus *Rhizophagus irregularis* was used to inoculate *L. japonicus* roots in a chive nurse plant system (based on Wegel

*et al.*, 1998). To prepare the nurse plants, *R. irregularis* spores (DAOM197198; Connectis, Agronutrition, Carbonne, France) were used to inoculate chive seedlings (c. 200 spores for 40 plants). *Rhizophagus irregularis* spores were collected by centrifugation at 805 g for 10 min at 4°C and resuspended in 10 ml of ¼-strength modified Hoagland's solution (based on the nitrogen-free medium described by Hoagland & Arnon (1938) with the following modifications: 1 mM KNO<sub>3</sub> and 100 µM KH<sub>2</sub>PO<sub>4</sub> added; replacing half of the chelated iron stock solution with 12.5 µM Fe-EDDHA). Chive seeds were briefly sterilized with 1.2% sodium hypochlorite (NaClO) and 0.1% sodium dodecyl sulphate (SDS) for 1–2 min and thoroughly washed with sterile distilled water. Pots used to grow chive plants were washed and sterilized with 70% ethanol before use. Sterilized chive seeds were placed on the surface of a sterile sand-vermiculite mixture (2 : 1) in a pot and watered with 35 ml of ¼-strength modified Hoagland's solution and 10 ml spore suspension. Chive pots were kept in a growth chamber (24°C, 16 h : 8 h, light : dark; light intensity of 180 µmol m<sup>-2</sup> s<sup>-1</sup>) and were covered with a plastic lid for the first 3 d. Chive plants were watered with ½-strength modified Hoagland's solution three times a week (20 ml solution for each pot). Six weeks post-inoculation, chive roots were stained to verify AM colonization. Two chive plants were transferred to a new pot containing a sterile sand-vermiculite mixture and 40 ml of 1/12-strength modified Hoagland's solution and allowed to grow for another 4–6 wk before being used as nurse plants. The shoot systems of chive nurse plants were cut off for AM inoculation experiments, leaving only colonized roots in the growth substrate.

### Plant growth conditions and phenotypic analysis

Seeds were scarified and surface-sterilized as previously described (Groth *et al.*, 2010) and plated on 1/2 Gamborg's B5 with 0.8% Bacto™ agar plates (Becton, Dickinson & Co., Heidelberg, Germany). Seeds were kept in the dark in a Panasonic growth chamber 24°C for 3 d and then on a 16 h : 8 h, light : dark. For phenotypic analysis under symbiotic condition (Figs 1, 2, S1, S2b–d), 10-d-old seedlings were transferred to Weck jars (SKU745; J. Weck GmbH u. Co. KG, Wehr-Öffingen, Germany) containing 300 ml of sterile sand : vermiculite mixture (2 : 1) wet with 30 ml of FAB medium containing *M. loti* DsRed. Roots were harvested indicated days post-inoculation (dpi) stated in the figure legends and the number of nodules was quantified. Roots harvested 3, 7 and 21 dpi were subjected to *GUS* staining as described in Groth *et al.* (2010) with the incubation time of 6 h (Figs 1, 2, S2c,d) to detect *GUS* activity. For phenotypic analysis under nitrogen-sufficient conditions (Fig. S2a), 7-d-old seedlings were transferred to Weck jars containing 300 ml Seramis : vermiculite mixture (4 : 1) wet with 30 ml of the nitrogen-containing version of ¼ Hoagland's solution (15 mM KNO<sub>3</sub>). Plants were harvested at 24 d post transfer. Shoot height was evaluated as the distance between the youngest leaves to the end of the hypocotyl. Root length was measured as the length of the whole root system, while shoot dry weight was measured as after shoots were dried at 60°C for 1 h in an incubator. For

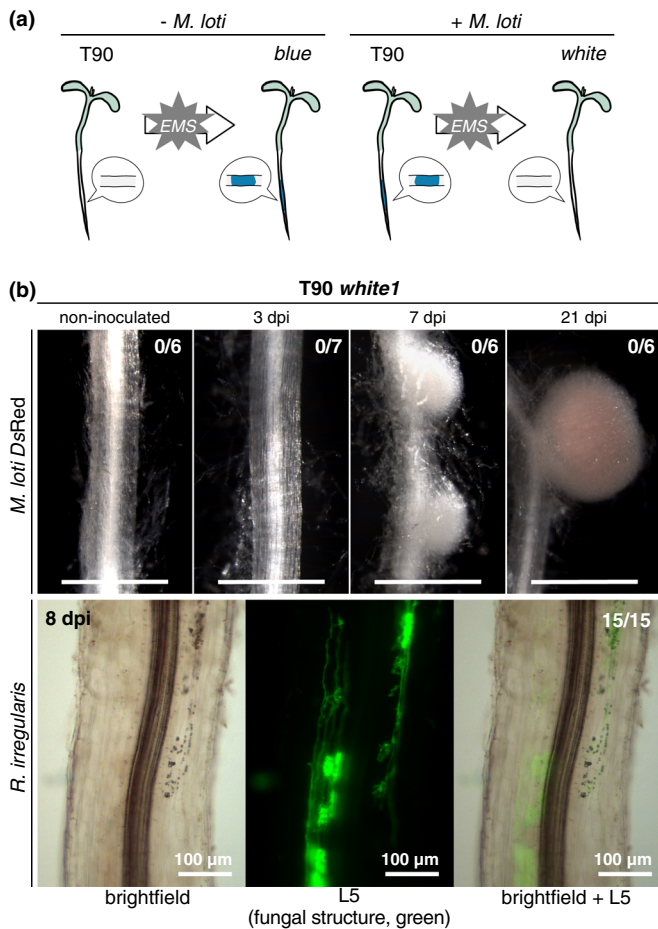


**Fig. 2** Absence of GUS activity in T90 *white* mutant roots during arbuscular mycorrhiza (AM) or root nodule symbiosis (RNS). (a) Schematics of the two screens of ethyl methanesulphonate (EMS)-induced mutant populations for  $M_2$  seedlings with altered GUS activity: spontaneous activation of the *GUS* gene in the absence of symbionts (left) or undetectable GUS activity in the presence of symbionts (right; resulting mutants are referred to as T90 *white* mutants). (b) T90 *white1* roots were stained with 5-bromo-4-chloro-3-indolyl- $\beta$ -D-glucuronic acid (X-Gluc) to reveal GUS activity at indicated days post-inoculation (dpi) with *Mesorhizobium loti* expressing *Discosoma* sp. red fluorescent protein (*M. loti* DsRed) or *R. irregularis*. Note the total absence of GUS activity in T90 *white* roots, compared to those of T90 upon inoculation with microsymbionts (tested side-by-side in the same experiment; see Fig. 1a, Supporting Information Fig. S1). Pictures of T90 *white1* root systems and analysis of T90 *white3* are included in Fig. S2(c,d). Green, Alexa Fluor-488 wheat germ agglutinin (WGA)-stained *R. irregularis* visualized with a Leica Filter Cube L5 next to a brightfield image of the same root segment. #/#, number of plants displaying GUS activity/total number of plants analysed. Bars, 1 mm unless stated otherwise.

promoter analysis (Figs 3, 6 (see later), S4, S7, S8), plants with transformed roots were transferred to either Weck jars containing 300 ml of sterile sand : vermiculite mixture (2 : 1) and 60 ml FAB medium containing *M. loti* DsRed; or chive nursing pots and watered with 1/4-strength modified Hoagland's solution (see the 'Plant, bacterial and fungal material' section earlier; with  $KNO_3$  increased to 9 mM) three times a week. Plants were grown under the same conditions as described for chive plants. For detecting *GUS* expression induced by ectopically expressed CCaMK<sup>T265D</sup>

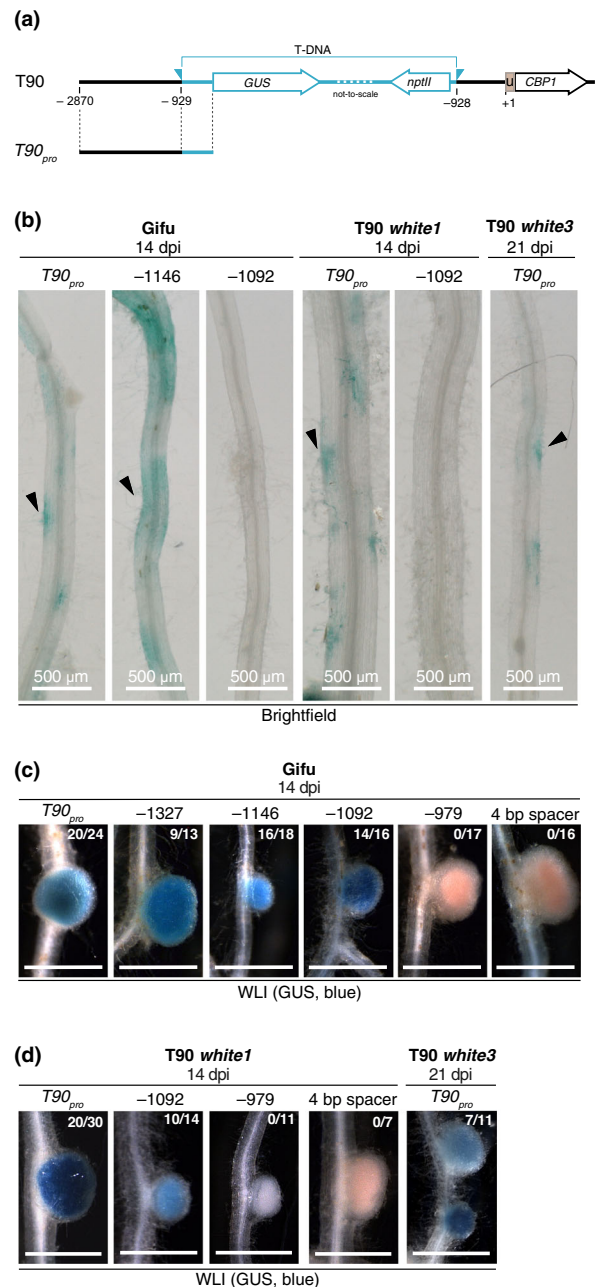


**Fig. 3** Absence of GUS activity in T90 *white* mutants can be restored by transgenic  $T90_{pro}$ :*GUS* fusions. (a) T-DNA insertion in the T90 line as in Fig. 1, here including the *CBP1* promoter reference coordinates used for definition of the length of the individual fragments tested in the T90 promoter deletion series (for symbols refer to Fig. 1b). (b–d) *Lotus japonicus* Gifu, or T90 *white* mutants (*white1* or *white3*) hairy roots transformed with T-DNAs carrying a  $Ubq10_{pro}$ :*NLS-GFP* transformation marker together with a *GUS* reporter gene driven by the full length T90 promoter (–2870) or a deletion series thereof (starting at –1327, –1146, –1092 or –979 of the *CBP1* promoter), or a 4 bp spacer sequence were analysed at indicated with *Mesorhizobium loti* expressing *Discosoma* sp. red fluorescent protein (*M. loti* DsRed). Images in (b) were obtained from the same set of root systems as in (c, d). Pictures of entire root systems from these experiments are included in Supporting Information Fig. S4 (a,b). #/#, number of plants showing GUS activity in nodules/total number of transgenic root systems analysed. Black arrowheads, blue patches in the root epidermis. Bars, 1 mm unless stated otherwise. WLI, white light illumination.

(Fig. S3), plants were grown in the absence of symbionts. A subset of plants, whose roots were transformed with *Ubi<sub>pro</sub>:CCaMK<sup>T265D</sup>-GFP* (Maekawa *et al.*, 2008; Yano *et al.*, 2008) or *Ubi<sub>pro</sub>:GW-GFP* (Maekawa *et al.*, 2008), were subject to GUS staining for 18 h at 37°C and 22 and 5 d post-transformation, respectively. The rest of plants were grown in sand : vermiculite mixture (2 : 1) and the spontaneous nodules induced on the transformed roots were observed 60 d post transformation. All transformed roots expressing *CCaMK<sup>T265D</sup>* formed spontaneous nodules regardless of the plant genotype.

### Promoter analysis and microscopy

*Lotus japonicus* hairy roots were generated using an *Agrobacterium rhizogenes* (Charpentier *et al.*, 2008) with the following modifications: (1) roots of seedlings were cut away while seedlings were immersed in *A. rhizogenes* that was re-suspended in sterile MilliQ water; (2) after removal of roots, shoots of the seedlings were transferred to plates containing Gamborg's B5 medium (without sucrose) and 0.8% BD Bacto™ agar. The T-DNA region of the construct carried in *A. rhizogenes* contained a green fluorescent protein (GFP) transformation marker (*Ubi10<sub>pro</sub>:NLS-2xGFP*) and a promoter : GUS reporter fusion placed in tandem. Chimeric root systems with transformed roots and/or nodules were identified by GFP fluorescence emanating from nuclei under a Leica MZ16 FA fluorescent stereomicroscope equipped with a GFP3 filter (excitation filter BP 470/40, suppression filter BP 525/50; Leica, Wetzlar, Germany). Transformed nodule primordia and nodules were identified by the presence of a red fluorescence signal under a *DsRed* filter 10–14 dpi, then excised and subject to GUS staining for 3 h at 37°C (Groth *et al.*, 2010, with incubating time adjusted). The whole root systems were subject to GUS staining for 6 h (Figs 3, S4, S6–S8, see later). For promoter analysis of mycorrhized roots, roots were subject to GUS staining for 14–16 h at 37°C, followed by staining with wheat germ agglutinin (WGA) (Methods S1). Microscopic procedures are detailed in Methods S2.

### DNA constructs

A detailed description of the constructs used in this study is provided in Table S2. Constructs were generated with the Golden Gate cloning system (Binder *et al.*, 2014). A variant of the *GUS* gene, *DoGUS* (from plasmid C204, DNA Cloning Service), used for cloning was kindly provided by David Chiasson (SMU, Halifax, Canada). Key plasmids were deposited to Addgene (plasmid ID listed in Table S2; <https://www.addgene.org>).

### EMS mutagenized T90 population and mutant screening

Generation of the EMS-mutagenized T90 population is described in the *L. japonicus* handbook section 'EMS mutagenesis' (Márquez, 2005). Details of plant growth procedure and screening are listed in Methods S3.

### Transient expression assays in *Nicotiana benthamiana* leaves

*Nicotiana benthamiana* plants were grown as previously described (Ceri *et al.*, 2017), and infiltration of *N. benthamiana* leaves with *A. tumefaciens* was performed as previously described (Ceri *et al.*, 2012) but with acetosyringone concentration modified to 150 µM. *Agrobacterium tumefaciens* carrying promoter : GUS fusion constructs of interest (strain AGL1) were co-infiltrated with *A. tumefaciens* containing plasmid *35S<sub>pro</sub>:3xHA-Cyclops* (strain AGL1; Singh *et al.*, 2014), *35S<sub>pro</sub>:CCaMK<sup>1-314</sup>-NLS-mOrange* (strain GV3101; Takeda *et al.*, 2012) or *35S<sub>pro</sub>:CCaMK<sup>T265D</sup>-3xHA* (strain GV3101; Yano *et al.*, 2008) as indicated in Figs 5 (see later) and S6. An AGL1 strain carrying a K9 plasmid constitutively expressing *DsRed* was used as needed to equalize the *A. tumefaciens* amount infiltrated per leaf, together with a strain carrying a plasmid for the expression of the viral P19 silencing suppressor (Voinnet *et al.*, 2003). *Nicotiana benthamiana* leaf discs with a diameter of 0.5 cm were harvested 60 h post infiltration. A total number of four to eight leaf discs per indicated vector combination were analysed in at least two independent experiments performed in different weeks.

### Quantitative fluorometric GUS assay and analysis

*Nicotiana benthamiana* leaf discs were subject to a quantitative fluorometric GUS assay (Jefferson, 1987) adapted for a 96-well plate format.

### Genomic DNA extraction and investigation of promoter methylation pattern

Roots (*c.* 100 mg) from plants grown in the absence of symbiont of each genotype were harvested, frozen and ground in liquid nitrogen with mortar and pestle. Genomic DNA (gDNA) was extracted as previously described (Lueders *et al.*, 2004). Concentration of gDNA was determined with a Nanodrop photometer (DS-11; DeNovix Inc., Hesse/Oldendorf, Germany). In total, 25 ng gDNA was subjected to restriction digestion by *Hae*II (NEB, Frankfurt, Germany) in a 10 µl reaction that contained 1 µl NEB Cutsmart restriction buffer (supplied with the enzyme), 1 µl gDNA, 1 µl (*c.* 10 units) of enzyme and 7 µl MilliQ water for 18 h at 37°C. PCR was performed with 1 µl of digestion mix as template and the primer pair 5'-AATAGTG GCATATGAAAATGTTGG-3' (F1) and 5'-AATTATAGGAA GACGTTGGAGAGT-3' (R1; Fig. 5, see later) to amplify a 218 bp region in the T90 promoter containing a single recognition site of each of the enzymes, or the primer pair 5'-TTTCGCCGATATCGTAGAC-3' and 5'-GCAACACCGG CTATATAATAGTG-3' to amplify a 198 bp region of the NIN promoter that does not contain recognition sites for any of the enzymes, as a control for the quality of digested gDNA. The PCR was performed with *Taq* DNA polymerase (catalogue no. M7848; Promega, Madison, WI, USA) as follows: initial denaturation at 95°C for 3 min, 30, 35 or 40 cycles of amplification (95°C for 20 s, then 53°C for 30 s, followed by 72°C for 25 s);

and a final extension step at 72°C for 5 min. PCR products were detected using agarose gel electrophoresis (2.0% agarose gel with 9.5 V cm<sup>-1</sup> for 40 min for Fig. 4; 1.0% agarose gel with 8 V cm<sup>-1</sup> for 35 min for Fig. S5).

### In silico prediction of transcription factor binding sites

The binding sites were predicted by TOMTOM (v.5.4.1; <https://meme-suite.org/meme/tools/tomtom>). The *EPRE<sub>CBP1</sub>* was used as input query motifs against the JASPAR (nonredundant) core plant database (2018). The motif column comparison function was Pearson correlation coefficient and a significance threshold of *E*-value < 10 was used. The identified putative motif sequences and corresponding known motif are summarized in Table S3.

### Data visualization and statistical analysis

Statistical analyses and data visualization were performed with RSTUDIO 1.1.383 (RStudio Inc., Boston, MA, USA). Boxplots were used to display data in Figs 5, S2 and S6 (Wickham & Stryjewski, 2011). The box indicates the interquartile range (IQR); Whiskers show the lowest/highest data point within 1.5 IQR of the lower/upper quartile. Black circles and numbers outside of the plotting area indicate data points outside 1.5 IQR of the upper quartile and the value of an individual data point outside of the plotting area, respectively. Bold black lines indicate median. Individual data points shown as unfilled circles were added to boxplots using R package BEESWARM (<https://github.com/aroneklund/beeswarm>). R package AGRICOLAE (Mendiburu, 2018) was used to perform ANOVA statistical analysis with *post hoc* Tukey. Statistical results were presented in small letters where

different letters indicate statistical significance, while overlapping letters indicate no significant statistical difference.

## Results

### T90 *white* mutants were identified from an EMS-mutagenized T90 population

In our hands, *GUS* expression in the T90 line behaved exactly as described earlier by Webb *et al.* (2000) and Kistner *et al.* (2005) (Figs 1b, S1). In response to *M. loti* inoculation, T90 features two characteristic transient *GUS* expression patterns: (1) at early stages in patches of epidermal cells before nodule appearance; (2) in the cortex during nodule initiation and development. The latter was reduced or absent in mature nodules (Fig. 1b). Sectioning of the root at 3 dpi revealed that the blue epidermal patches can be associated with underlying blue cortical cells (Fig. S1b). In response to AM fungus *R. irregularis*, *GUS* expression was predominantly observed in cortical tissue colonized by the fungus (Fig. 1b).

To identify the regulators of the T90 *GUS* gene, we performed two independent forward genetic screens. The rationale was as follows: mutants with altered *GUS* activity (and/or impaired symbiotic behaviour) likely possess defects in the regulatory machinery that directly or indirectly regulate the transcription of the *GUS* gene. Given that transcriptional activation of the *GUS* gene in T90 occurs in response to symbiotic interactions, these impaired machineries potentially regulate gene expression in AM and/or RNS. An EMS-mutagenized T90 M<sub>2</sub> population was generated by separately harvesting seeds of 1342 M<sub>1</sub> plants labelled T0001–T1342. Two independent screens were conducted at the seedling stage utilizing individual M<sub>2</sub> families to

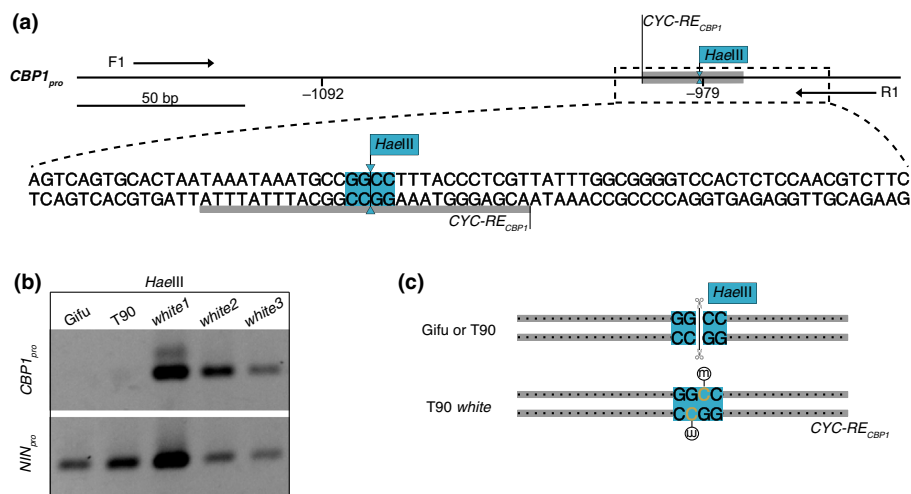


**Fig. 4** Cytosine methylation within a 113 bp T90 promoter region of T90 *white* mutants but not those of T90 or *Lotus japonicus* Gifu. (a) Genomic DNA (gDNA) from *L. japonicus* Gifu, T90 or T90 *white* mutants (*white1*, *white2* or *white3*) was digested with the methylation-sensitive restriction enzyme *HaellI*. Blue shade on DNA sequence, recognition site of *HaellI*. Grey shade in the restriction map or grey underline of promoter sequence, *CYC-RE<sub>CBP1</sub>*. Arrowheads and lines, endonucleolytic cleavage site and outline of the restriction digestion products. (b) Analysis of the success of restriction digestion by PCR. Digested gDNA from the indicated genotype was used as a template for PCR amplification with primers F1 and R1 flanking a 218 bp promoter region (upper panel) and primers flanking a 198 bp stretch of the *L. japonicus* *NIN* promoter as control (lower panel). This region in the *NIN* promoter does not contain the restriction site for *HaellI*. Note that PCR products could be obtained using digested gDNA from the T90 *white* mutants but not from Gifu or T90 as the amplification template. (c) Graphic summary of the results in (b) projected onto the promoter region together with the recognition sites of *HaellI*. m in an open circle, methyl groups; Scissor cartoon, successful endonucleolytic cleavage.

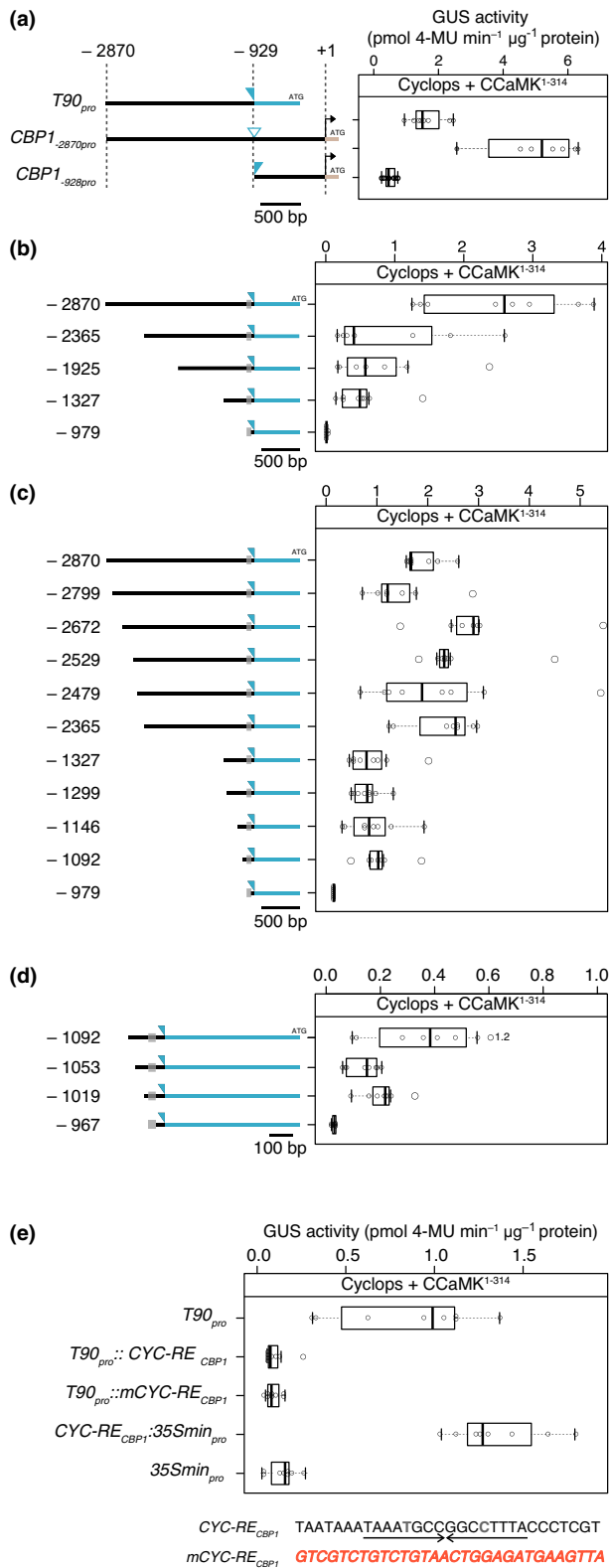


**Fig. 5** A *cis*-element in the promoter of *CBP1* is necessary and sufficient for the CcCaMK<sup>1–314</sup>/Cyclops-mediated transactivation of promoter: *GUS* reporter fusions in *Nicotiana benthamiana* leaf cells. (a–e) *Nicotiana benthamiana* leaf cells were transformed with T-DNAs carrying a *GUS* reporter gene driven by either of the indicated promoters: (a) the *T90<sub>pro</sub>* promoter (labelled as *T90<sub>pro</sub>* in a, d or –2870 in b, c); one of the two *CBP1* promoter regions (*CBP1*<sub>–2870<sub>pro</sub></sub> or *CBP1*<sub>–928<sub>pro</sub></sub>); (b–d) promoter deletion series generated in the context of *T90<sub>pro</sub>* including promoter regions that were (b) c. 300–500 bp different in length, (c) c. 50–100 bp different in length within –2870 to –2365 bp or –1327 to –979 bp, (d) c. 35–50 bp different in length within –1092 to –967 bp; (e) *T90<sub>pro</sub>*, *T90<sub>pro</sub>* with the 30 nt long *cis*-element (*CYC-RE<sub>CBP1</sub>*) mutated or deleted (*T90<sub>pro</sub>::mCYC-RE<sub>CBP1</sub>* or *T90<sub>pro</sub>::ΔCYC-RE<sub>CBP1</sub>*, respectively), a 35S minimal promoter (*35Smin<sub>pro</sub>*), or *CYC-RE<sub>CBP1</sub>* fused to *35Smin<sub>pro</sub>* (*CYC-RE<sub>CBP1</sub>::35Smin<sub>pro</sub>*). The numbers in (a–d) indicating length of promoter were based on *CBP1* promoter taking its transcriptional start site as +1. Left of the boxplots in (a–d) are graphic illustrations of the promoter regions driving the *GUS* reporter gene with the open triangle and grey boxes illustrating the T-DNA insertion site projected onto the *CBP1* promoter and of *CYC-RE<sub>CBP1</sub>*, respectively. Black and blue colour label regions originating from the *Lotus japonicus* wild-type genome and from the T-DNA in *T90*, respectively. The larger experimental set-up boxplots including the results of negative controls is presented Supporting Information Fig. S4 with statistical tests. Note the palindromic sequence within the *CYC-RE<sub>CBP1</sub>* highlighted by opposing arrows. Interrupted by only two nonmatching basepairs highlighted in grey and bold.

indolyl-β-D-glucuronic acid (X-Gluc) whereas the rest of the seedling was maintained to allow for seed production and analysis of heritability. Screen A of 519 M<sub>2</sub> and 203 M<sub>3</sub> lines resulted in 84 plants from 55 lines which showed spontaneous *GUS* expression in the roots, however no progenies from them inherited this phenotype. Screen B of 709 M<sub>2</sub> lines for loss of *M. loti*-induced *GUS* activity, resulted in three lines that exhibited heritable aberrant *GUS* phenotypes. In detail, three M<sub>2</sub> plants (L8668 and L8686–8687, progeny from M<sub>1</sub> plant T614 and T1305, respectively), were identified that did not exhibit blue staining after incubation with *M. loti*. Based on the white colour of their roots after *GUS* staining, these three plants were renamed *T90 white* mutants (L8668 *white1*, L8686 *white2* and L8687 *white3*) and allowed to self-fertilize. The progeny of all three *T90 white* plants displayed normal shoot and root morphology and could successfully establish AM and RNS similarly as *T90* and *L. japonicus* Gifu (Fig. S2a,b), however *GUS* activity could not be detected in their roots during both symbioses (Figs 2b, S2c,d). *T90 white2* was less healthy than *white3* and produced limited seeds at the time of this study; therefore, only the progeny of *T90 white3* was included in some subsequent experiments.

### *T90 GUS* expression is genetically located downstream of the common symbiosis genes

All three *T90 white* mutants were able to establish both RNS and AM without apparent defects, indicating that essential genes for establishment of symbioses were intact. We sequenced the endogenous *GUS* gene in *T90 white* mutants and did not detect alterations in its coding sequences, hence ruling out that mutations in the endogenous *GUS* genes caused the *T90 white*

identify (A) individual M<sub>2</sub> plants displaying spontaneous activation of the *GUS* gene in the absence of symbionts or (B) individual M<sub>2</sub> plants with altered *GUS* activity in presence of *M. loti* (Fig. 2a; for further details see Tuck, 2006). For this purpose, root pieces were removed and stained with 5-bromo-4-chloro-3-

phenotype. For the cause of T90 *white* phenotype, we considered two possible scenarios: (1) a pathway independent of essential symbiosis genes is involved in activation of the T90 *GUS* gene, which is defective in T90 *white*; (2) the regulatory region of the *GUS* gene is defective in T90 *white* leading to aberrant *GUS* gene induction. To investigate these possible scenarios, we sought to resolve the connection of the transcriptional activation of the T90 *GUS* gene to that of symbiosis signalling by crossing the T90 *GUS* insertion into homozygous backgrounds for mutant alleles of common symbiosis genes. These included mutant allele *ccamk-2* for *CCaMK* (line *cac57.3*; Perry *et al.*, 2009), *symrk-10* for *SymRK* (Perry *et al.*, 2003), *nfr1-1* for the nod factor receptor gene *Nod Factor receptor 1 (NFR1)* (Radutoiu *et al.*, 2003) and *pollux-1* for the cation channel *Pollux* (EMS70; Szczyglowski *et al.*, 1998). Preliminary results showed that the F<sub>2</sub> plants from the following crosses, *ccamk-2* × T90, *nfr1-1* × T90 and T90 × *symrk-10* (Gossmann *et al.*, 2012) did not respond with *GUS* expression after *M. loti* inoculation. Based on these findings, we concluded that the T90 *GUS* gene expression is dependent on the tested genes, and positioned the transcriptional activation of the T90 *GUS* gene downstream of *NFR1*, *SymRK*, *Pollux* and *CCaMK*. Consistent with this model, ectopically expressed *SymRK* in T90 hairy roots was able to induce the T90 *GUS* expression (Ried *et al.*, 2014).

We tested whether the T90 *GUS* gene expression can be activated by transgenically expressed autoactive *CCaMK*<sup>T265D</sup> in T90 and T90 *white* mutants' hairy roots. These T90 hairy roots spontaneously induced *GUS* expression in the absence of a microsymbiont (Fig. S3).

Importantly, *A. rhizogenes*, a member of the Rhizobiaceae and frequently used for hairy root transformation, did not induce the *GUS* expression in T90 (Gossmann, 2011), supporting that the observed spontaneous *GUS* induction resulted from transgenically expressed *CCaMK*<sup>T265D</sup>. By contrast, we did not observe spontaneous induction of *GUS* expression by *CCaMK*<sup>T265D</sup> in T90 *white1* and T90 *white3* hairy roots (Fig. S3). These data provide independent evidence for the position of the T90 *GUS* expression downstream of *CCaMK*. The observation that T90 but not T90 *white* mutants responded with *GUS* expression to autoactive *CCaMK*<sup>T265D</sup> combined with the fact that *CCaMK* phosphorylates and interacts with Cyclops for activation of downstream genes during symbiosis (Singh *et al.*, 2014; Pimprikar *et al.*, 2016; Cerri *et al.*, 2017), motivated us to investigate a possible involvement of Cyclops in the T90 *white* phenotype. We therefore sequenced *Cyclops* in T90 *white* mutants to test for the unlikely case that mutations in the gene prevented *GUS* genes induction, without influencing symbiosis *per se*. We did not detect any sequence alterations of the *Cyclops* gene in all three mutant lines.

### Transgenic insertion of a T90 promoter : *GUS* fusion in the T90 *white mutant* background restored symbiosis-inducible *GUS* expression

Based on the observed dependency of T90 *GUS* expression on genes involved in early symbiotic signalling, together with the

success of T90 *white* to form both RNS and AM, we hypothesized that these symbiosis genes are likely functional in T90 *white*. We consequently redirected our focus onto the regulatory region of the T90 *GUS* gene. To this end we cloned a chimeric region of 2530 bp directly 5' of the *GUS* gene in T90, hereafter called 'T90 promoter'. This region comprised a 1942 bp fragment positioned between -2870 bp to -929 bp relative to the transcriptional start site of *CBP1*, followed at the 3' end by 588 bp of the T-DNA sequence 5' of the ATG of the *GUS* gene (Fig. 3a). This fusion is identical to the original T90 fusion and contains all elements necessary for the transcription of the *GUS* gene, such as a minimal promoter and a transcriptional start site (Jefferson *et al.*, 1987; Topping *et al.*, 1991). We transformed *L. japonicus* Gifu hairy roots with T-DNAs containing a *GUS* reporter gene driven by the T90 promoter (*T90<sub>pro</sub>:GUS*) and analysed the *GUS* expression in the transgenic roots followed by inoculation with *M. loti* *DsRed*. Upon exposure of roots to X-Gluc, blue staining indicative of *GUS* expression was detected exclusively in two areas: (1) in distinct patches each composed of multiple root epidermal cells (Fig. 3b; compare to the T90 pattern in Fig. S1); (2) in the central tissue of nodules (Figs 3c, S4a). The remarkable 'blue epidermal patches' could differ strongly in size and definitively involved epidermal cells as evidenced by the blue colour detected in root hairs and the blue colour in the basis of epidermal cells (Fig. 3b). However, given the spatio-temporal dynamics of their appearance and disappearance, we did not determine contribution of outer cortical cell layers to these blue patches. Taken together, the staining pattern observed for *T90<sub>pro</sub>:GUS* transgenic hairy roots matched key aspects observed for the T90 line (Figs 1b, S1). By contrast, *T90<sub>pro</sub>:GUS*-transformed roots grown in the absence of microsymbionts or roots transformed with an identical construct in which the T90 promoter was replaced by a 4 bp spacer sequence did not exhibit any blue staining (Figs 3c, S4a).

We sequenced the corresponding T90 promoter region of the three T90 *white* mutants and could not detect any sequence alteration (data not shown). We consequently hypothesized that these mutants may suffer from an epigenetic change that renders its corresponding T90 promoter region nonfunctional. To test this hypothesis, T90 *white1* and *white3* hairy roots were transformed with the *T90<sub>pro</sub>:GUS* reporter fusion construct and analysed for *GUS* expression. In the absence of microsymbionts, no blue staining was detected. After inoculation with *M. loti* *DsRed*, blue staining could be observed in both areas characteristic for T90: patches of root epidermal cells (Fig. 3b) and in the inner tissue of nodules (Figs 3d, S4b). Hairy root transformation did not result in a revival of the T90 endogenous *GUS* gene, as T90 *white1* hairy roots transformed with a *GUS* reporter gene driven by a 4 bp spacer sequence did not exhibit any blue staining (Figs 3d, S4b). Because the endogenous *GUS* genes in the T90 *white* mutants were not induced during nodulation or hairy root formation, the blue staining could only result from expression of the introduced *T90<sub>pro</sub>:GUS* reporter fusion. These observations indicated that the machinery targeting the T90 promoter to induce gene expression during nodulation is intact in T90 *white* mutants and supported the hypothesis that epigenetic changes



block the expression of the endogenous *GUS* genes in T90 *white* mutants.

A 54 bp and a 113 bp region in the T90 promoter are required for tissue-specific expression

To further dissect the promoter and identify relevant regions and *cis*-elements, we generated 5' deletion series of the T90 promoter in the context of the *T90<sub>pro</sub>:GUS* reporter fusion (starting at -2870 bp relative to the *CBP1* transcriptional start site), without modifications of the rest of the promoter or reporter. The resulting individual constructs started at -1327, -1146, -1092 and -979 bp (Fig. 3c) and were introduced individually into *L. japonicus* Gifu or T90 *white1* hairy roots. We observed the characteristic blue patches of root epidermal cells on Gifu and T90 *white* roots transformed with the *GUS* reporter gene driven by *T90<sub>pro</sub>* or a shorter promoter -1146 bp (Fig. 3b). The epidermal blue staining pattern was no longer detected when a region -1092 bp was tested (Fig. 3b). This 54 bp region (-1146 to -1092 bp) was therefore called the 'Epidermal Patch Response Element in the *CBP1* promoter' (*EPRE<sub>CBP1</sub>*). Blue staining was observed in nodules transformed with either of the T90 promoter: *GUS* fusions starting at -1327, -1146 or -1092 bp (Fig. 3c, S4a). Further deletion to -979 bp, as well as promoter replacement with a 4 bp spacer sequence eliminated blue staining in nodules (Fig. 3c). An identical pattern was observed in hairy roots of T90 *white1* where a -1092 bp region could achieve *GUS* activity in transgenic nodules, but not a -979 bp region (Figs 3d, S4b). We concluded based on these findings that a region of 113 bp (-1092 to -979 bp) and a stretch of 54 bp located directly 5' (-1146 to -1092 bp; *EPRE<sub>CBP1</sub>*) was necessary for gene expression in nodules and the root epidermis, respectively.

T90 promoter hypermethylation was detected in three T90 *white* mutants

DNA methylation is an important and frequently occurring driver of epigenetic changes, which can attenuate binding by the transcription regulatory proteins, thereby inhibiting the activation of target genes (Medvedeva *et al.*, 2014; Yang *et al.*, 2020). We investigated whether an epigenetic event interfering with the endogenous *GUS* expression in T90 *white* mutants could be related to DNA methylation. To detect differences in the methylation pattern between T90 and T90 *white* mutants, we took advantage of the DNA restriction endonuclease *HaeIII* whose activity is impaired by cytosine methylation in its GGCC recognition site (rebase.neb.com). Its recognition site is present in the short 113 bp region, deletion of which led to a complete absence of *GUS* gene expression during nodulation (Fig. 3b). To detect differential methylation at this site, we performed restriction digestion of gDNA extracted from roots of *L. japonicus* Gifu, T90 and T90 *white* mutants grown in the absence of microsymbionts, followed by PCR. PCR-based amplification of a gDNA region containing a *HaeIII* recognition site and digested with *HaeIII* is only successful when its recognition site is methylated and thus protected from cleavage. A promoter region of the *NIN*

gene that did not contain any recognition site could be successfully amplified with digested gDNA from all genotypes, demonstrating that the gDNA quality was suitable for PCR after restriction digestion (Fig. 4b, lower panel). By contrast, a PCR product using the primers covering the *CBP1* promoter region displayed in Fig. 4(a) was only obtained using digested gDNA from T90 *white* mutants as the amplification template, but not with that from Gifu or T90 (Fig. 4b, upper panel). Amplicons for the latter two were also not detected when increasing the PCR amplification cycle to 35 or 40 (Fig. S5), indicating a complete *HaeIII* digestion of the gDNA. Embedded into the context of *CYC-RE<sub>CBP1</sub>*, the critical C for *HaeIII*'s methylation sensitivity falls into the CHH sequence pattern of cytosine methylation sites in plants, frequently associated with epigenetic transcriptional gene silencing (Iwasaki & Paszkowski, 2014). Taken together, the so discovered differential methylation within the *CYC-RE<sub>CBP1</sub>* is likely the cause for the loss of *GUS* expression in the T90 *white* mutants.

*CBP1* is regulated by the CCaMK/Cyclops complex

The observations that the T90 *GUS* gene expression can be induced by exposure to rhizobia and an AM fungus as well as spontaneously by autoactive CCaMK suggested that the T90 promoter is likely subject to CCaMK/Cyclops regulation. We used transient expression assays in *N. benthamiana* leaves to test whether the CCaMK/Cyclops protein complex could transcriptionally induce expression of a *GUS* reporter gene under the control of the *CBP1* promoter or the T90 promoter (Figs 5a, S6a,b). A 2870 bp region 5' of the transcriptional start site of *CBP1* was cloned together with the 177 bp 5' untranslated region (UTR) of *CBP1* from *L. japonicus* Gifu (*CBP1<sub>-2870pro</sub>*). The expression of the reporter gene driven by *T90<sub>pro</sub>* or *CBP1<sub>-2870pro</sub>* was induced in the presence of Cyclops and the autoactive CCaMK<sup>1-314</sup> (CCaMK<sup>1-314</sup>/Cyclops; Figs 5a, S6b). In addition, *T90<sub>pro</sub>* achieved transcriptional activation mediated by CCaMK<sup>T265D</sup>/Cyclops (Fig. S6a). A 928 bp stretch of *CBP1* promoter corresponding to the region 3' to the T90 T-DNA insertion site (*CBP1<sub>-928pro</sub>*; fused to the *CBP1* 5' UTR in the reporter fusion) did not achieve reporter gene induction by CCaMK<sup>1-314</sup>/Cyclops (Figs 5a, S6b). These observations together indicated the presence of putative *cis*-regulatory elements responsive to CCaMK/Cyclops-mediated transactivation between -2870 and -928 bp of the *CBP1* promoter.

*CBP1* promoter dissection revealed a novel Cyclops response *cis*-regulatory element

To identify the CCaMK/Cyclops-responsive *cis*-regulatory element, we generated a promoter 5' deletion series and investigated reporter gene activation by CCaMK<sup>1-314</sup>/Cyclops-mediated transactivation in transient expression assays in *N. benthamiana* leaves (Figs 5b-d, S6c-e). The 5' deletion series was built on the basis of *T90<sub>pro</sub>:GUS* (constructed in the same way as those tested in Fig. 3). Each construct comprises a *CBP1* promoter stretch of variable length. The nucleotide position at the 5' end of the

deletions is based on the coordinates of the *CBP1* promoter (see Fig. 1a). An initial comparison of the transactivation strength across the deletion series revealed a reduction to *c.* 50% when comparing  $-2780$  and  $-2365$  bp and a complete loss of activity when comparing  $-1327$  to  $-979$  bp (Fig. 5b), indicating that these two regions might contain the responsible *cis*-elements. Testing further deletions that were *c.* 100 bp different in length within these two regions revealed that the series between  $-2870$  and  $-2365$  exhibited large variations in responsiveness between replicates and was therefore not investigated further. In the  $-1327$  to  $-979$  series, fragments equal to or longer as  $-1092$  resulted in similar reporter gene activation mediated by CCaMK<sup>1-314</sup>/Cyclops, while construct  $-979$  was inactive, suggesting the presence of relevant *cis*-element(s) between  $-1092$  and  $-979$  bp (Figs 5c, S6c). By testing a higher resolution series with 35 bp to 50 bp length difference, we narrowed down the responsible *cis*-element to the 30 nucleotides between  $-997$  and  $-967$  bp that contained an almost perfect (only two nonmatching basepairs; Fig. 5e) palindromic sequence of 16 bp. We called this element 'Cyclops-response element within the *CBP1* promoter' (*CYC-RE<sub>CBP1</sub>*) because a loss of reporter gene induction by CCaMK<sup>1-314</sup>/Cyclops was observed when this element was deleted (Figs 5d, S6d). To test the relevance of *CYC-RE<sub>CBP1</sub>* in the context of the T90 promoter, we mutated or deleted *CYC-RE<sub>CBP1</sub>* (*T90<sub>pro</sub>::mCYC-RE<sub>CBP1</sub>* and *T90<sub>pro</sub>::ΔCYC-RE<sub>CBP1</sub>*, respectively). Both resulted in an almost complete loss of CCaMK<sup>1-314</sup>/Cyclops-mediated transcriptional activation, indicating that *CYC-RE<sub>CBP1</sub>* was essential for this transcriptional activation (Figs 5e, S6e). Moreover, *CYC-RE<sub>CBP1</sub>* fused to a 35S minimal promoter (*CYC-RE<sub>CBP1</sub>:35S<sub>min</sub><sub>pro</sub>*) was sufficient for the activation of reporter gene (Figs 5e, S6e). These results together indicated that *CBP1<sub>pro</sub>* (and *T90<sub>pro</sub>* in the context of T90 genome) is regulated by the CCaMK/Cyclops complex through a *cis*-regulatory element *CYC-RE<sub>CBP1</sub>*.

### *CYC-RE<sub>CBP1</sub>* drives gene expression during RNS and AM

*CYC-RE<sub>CBP1</sub>* is located only 39 bp 5' of the T-DNA insertion site in T90 and we noticed that *CYC-RE<sub>CBP1</sub>* sits within the hypermethylated region in the T90 *white* mutants (Fig. 3). Given the necessity and sufficiency of *CYC-RE<sub>CBP1</sub>* for CCaMK/Cyclops-mediated transcriptional activation (Fig. 5) as well as the common requirement of this protein complex in AM and RNS, we hypothesized that this *cis*-element might be responsible for the symbioses-specific *GUS* expression in T90. To test this, a *GUS* or *DoGUS* (a variant of *GUS*) gene driven by *CYC-RE<sub>CBP1</sub>* fused to a 35S minimal promoter (*CYC-RE<sub>CBP1</sub>:35S<sub>min</sub><sub>pro</sub>*) or the T90 promoter (*T90<sub>pro</sub>*) was introduced into *L. japonicus* Gifu hairy roots, followed by inoculation with *M. loti* DsRed or the AM fungus *R. irregularis* (Figs 6, S7). During nodulation, *GUS* activity in roots transformed with *CYC-RE<sub>CBP1</sub>:35S<sub>min</sub><sub>pro</sub>:GUS* exhibited blue staining specifically in nodule primordia and nodules, but not root hairs (Fig. 6a). By contrast, *T90<sub>pro</sub>:GUS*-transformed roots displayed a much broader *GUS* activity in epidermis including root hairs (see also Fig. S4c), in addition to that observed in nodule primordia and nodules (Figs 3a, 6a). The same

promoter: reporter fusions constructed with *DoGUS* instead of *GUS* led to similar results (Fig. S4c). During mycorrhization, blue staining was detected in segments in roots transformed with *T90<sub>pro</sub>:DoGUS* and correlated strongly with the presence of *R. irregularis*, at the entry site of fungal hyphae crossing the epidermis (Fig. S7) and in cortical cells containing arbuscules (Fig. 6b). Blue staining in roots transformed with *CYC-RE<sub>CBP1</sub>:35S<sub>min</sub><sub>pro</sub>:DoGUS* could be specifically detected in the cortex in segments of roots, where cells were infected by *R. irregularis* (Fig. 6b). In both cases, *GUS* activity was visibly stronger in cells that were just invaded or had developing arbuscules, compared to those that the arbuscules almost occupying the entire cells. By contrast, roots transformed with *GUS* or *DoGUS* driven by the 35S minimal promoter did not display *GUS* activity during RNS or AM. Roots transformed with either one of the mentioned fusion constructs grown in the absence of microsymbionts exhibited only rarely blue staining, and if so, in vasculature or root tips regardless of the reporter fusion. We concluded that *CYC-RE<sub>CBP1</sub>* confers AM- and RNS-related gene expression specifically in the fungal colonized root cortical cells and in nodules, respectively.

### The *CBP1* promoter drives gene expression during RNS

We observed that *CYC-RE<sub>CBP1</sub>* in the context of the T90 promoter mediated responsiveness to transactivation by CCaMK/Cyclops and conferred gene expression during symbioses. The T-DNA insertion in T90 physically separated the promoter of *CBP1* into two regions: one containing *CYC-RE<sub>CBP1</sub>* located 5' of the insertion (5' region) and the other 3' of the insertion (3' region). It has been hypothesized previously that the 5' region enhances *CBP1* expression during symbiosis while the 3' region was responsible for its basal expression (Tuck, 2006). To investigate the role of the 3' region in more detail, we generated *L. japonicus* Gifu hairy roots transformed with a *GUS* reporter gene driven by *CBP1<sub>-2870pro</sub>* that represents the 'native' full length promoter comprising both the 5' and the 3' region or *CBP1<sub>-928pro</sub>* consists of only the 3' region (Fig. 1b). Transgenic roots were analysed 14 or 21 dpi with *M. loti* DsRed for *GUS* expression (Fig. S8). *CBP1<sub>-2870pro</sub>:GUS*-transformed roots exhibited strong blue staining in nodules, vasculature tissue, lateral root primordia and root tips (93% of transgenic root systems displaying blue staining in nodules). In comparison, blue staining in *CBP1<sub>-928pro</sub>:GUS*-transformed roots was observed in the same tissue and organ types, however at a lower efficiency (*c.* 50% of transgenic root systems displaying blue staining in nodules), and the blue staining was overall visibly weaker in nodules. These observations were consistent with the hypothesis that the 5' region enhances *CBP1* expression during nodulation.

## Discussion

### The *CBP1* promoter comprises at least four expression-modulating regions

With the goal to uncover regulatory elements involved in symbiosis, we investigated regulatory circuits underlying the

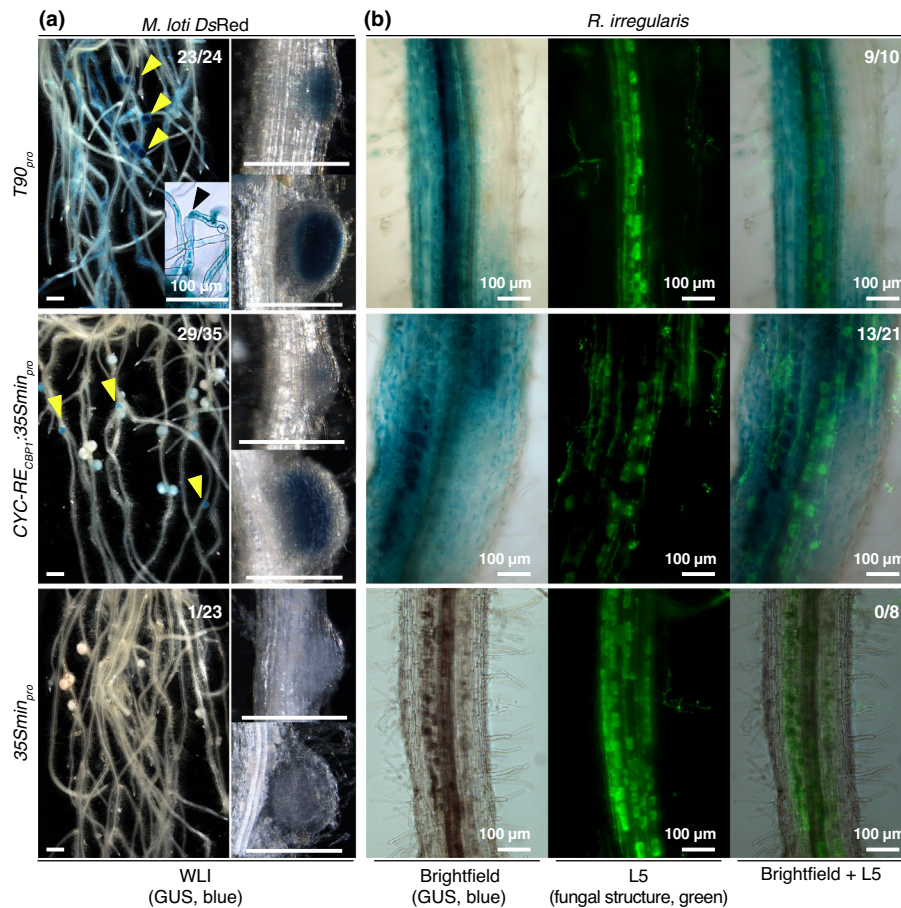


**Fig. 6** Spatio-temporal *GUS* expression driven by  $CYC-RE_{CBP1}$  in *Lotus japonicus* hairy roots during nodulation and mycorrhization. *Lotus japonicus* Gifu hairy roots were transformed with T-DNAs carrying a  $Ubq10_{pro}:NLS-GFP$  transformation marker together with a *GUS* reporter gene driven by the either of the following promoters: the T90 promoter ( $T90_{pro}$ ), a 35S minimal promoter ( $35Smin_{pro}$ ), or  $CYC-RE_{CBP1}$  fused to  $35Smin_{pro}$  ( $CYC-RE_{CBP1}:35Smin_{pro}$ ). Transformed roots and nodules were analysed (a) 10–14 days postinoculation (dpi) with *Mesorhizobium loti* expressing *Discosoma* sp. red fluorescent protein (*M. loti DsRed*) or (b) 12 dpi with *Rhizophagus irregularis*. Note that *GUS* activity was detected in root hairs (black arrowhead in a) in the roots transformed with  $T90_{pro}:GUS$  but not with  $CYC-RE_{CBP1}:35Smin_{pro}:GUS$  (for additional support see Supporting Information Fig. S4c). Overall,  $T90_{pro}:GUS$  gave stronger *GUS* activity (i.e. darker blue colour) in nodules than  $CYC-RE_{CBP1}:35Smin_{pro}:GUS$  (yellow arrowheads; compare the overview images of root systems). Note that  $35Smin_{pro}:GUS$  did not show any *GUS* activity during nodulation or mycorrhization except for *GUS* activity in vasculature in rare cases. Green, Alexa Fluor-488 WGA-stained *R. irregularis* visualized with a Leica Filter Cube L5 next to a brightfield image of the same root segment. #/#, number of plants showing *GUS* activity in nodules or root cortex/total number of transgenic root systems analysed. Bars, 1 mm unless stated otherwise.

symbiosis-specific *GUS* expression of the *L. japonicus* promoter tagging line T90. We observed that the T90 *GUS* expression can be largely recapitulated in hairy roots transformed with a *GUS* reporter gene driven by a region between  $-2870$  and  $-967$  bp of the *CBP1* promoter fused to the same T-DNA border found in the genomic arrangement of the T90 line. The expression pattern achieved by this region matches all key aspects of that of the T90 line: in root hairs and nodules in presence of *M. loti*; as well as root epidermis and cortical cells when roots were colonized by an AM fungus; and in both symbioses, absent from other tissues such as root vasculature and root tips. We therefore used this transgenic setting as the starting point to dissect the promoter function using a classical promoter deletion series. Our analysis revealed at least four regions/elements with significant impact on *CBP1* expression (Fig. 7). First, a 30 bp  $CYC-RE_{CBP1}$  is essential for gene expression in nodules and root cortex: we identified a 30-nucleotide long element named  $CYC-RE_{CBP1}$  within the

region  $-997$  and  $-967$  bp which is only 39 bp 5' of the T-DNA insertion in T90 (Fig. 7). This element, when equipped with a minimal promoter, was able to confer gene expression during both RNS and AM (Fig. 6), specifically in nodules and infected cortical cells, respectively. The features of  $CYC-RE_{CBP1}$  provide a plausible explanation for the common and symbioses-specific *GUS* activity in T90: as a result of the T-DNA insertion in T90, the promoterless *GUS* gene was coincidentally brought in proximity at the 3' of  $CYC-RE_{CBP1}$ , a *cis*-element that drives gene expression during colonization by rhizobia and AM fungi. In the presence of microsymbionts, the *GUS* gene was consequently activated generating a symbioses-specific expression pattern. By performing transactivation assays in *N. benthamiana* leaves, we observed that  $CYC-RE_{CBP1}$  equipped with a minimal promoter was sufficient for CCaMK/Cyclops-mediated transcriptional activation (Fig. 5e). Our results provide evidence of the involvement of CCaMK/Cyclops in mediating activation of the *CBP1* gene

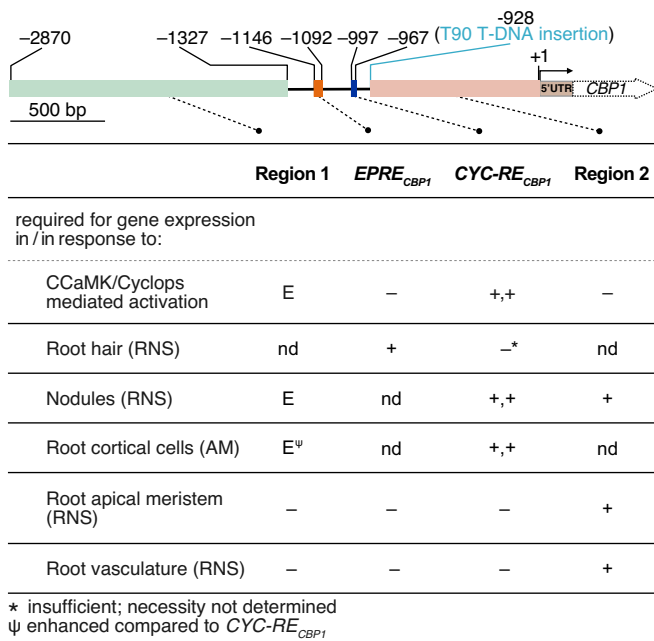


**Fig. 7** Four regulatory regions of the *CBP1* promoter and their impact on gene expression. *EPRE*<sub>*CBP1*</sub> and *CYC-RE*<sub>*CBP1*</sub> confer tissue specificity while region 1 and region 2 contribute to the expression strength of the *CBP1* gene. +, necessary; -, not necessary; E, enhancing expression strength; +,+, necessary and sufficient; nd, not determined. Note that the quality attribute 'necessary' is based on results obtained in different promoter contexts. For *EPRE*<sub>*CBP1*</sub> and *CYC-RE*<sub>*CBP1*</sub>, this annotation is based on the T90 promoter context and region 2 may contain at least partially redundant functions. The entire promoter and 5' UTR are drawn to scale, while *CBP1* (dotted arrow) it is not.

encoding a putative calcium-binding protein for both RNS and AM, through a common *cis*-element *CYC-RE*<sub>*CBP1*</sub>. In *L. japonicus*, the expression of the endogenous *CBP1* during nodulation in roots is likely enhanced by the presence of *CYC-RE*<sub>*CBP1*</sub> in its promoter (Fig. S8). This conclusion is based on the fact that *CBP1* is expressed at a reduced level in T90 roots in which the T-DNA insertion presumably reduces or entirely blocks the activity of this *cis*-element (Webb *et al.*, 2000). Second, a 54 bp region 5' of *CYC-RE*<sub>*CBP1*</sub> (*Epidermal Patch Response Element* (*EPRE*<sub>*CBP1*</sub>)) positioned between -1146 and -1092 bp is essential for *GUS* expression in patches of root epidermal cells in proximity to or undergoing IT formation (Fig. 3c). Expression in root epidermal cells could not be achieved when the region was deleted from the T90 promoter or when *CYC-RE*<sub>*CBP1*</sub> was tested on its own. Whether this region is required for epidermal expression achieved by T90 promoter during AM development (Fig. S7) requires a refined analysis of early infection stages. Moreover, *in silico* analysis predicts a number of transcription factors that potentially bind to *EPRE* (Table S3), the involvement of which in *CBP1* regulation remains to be investigated. Third, the region 3' of the *CYC-RE*<sub>*CBP1*</sub> is boosting CCaMK/Cyclops-mediated expression: the region 3' of *CYC-RE*<sub>*CBP1*</sub>, between -928 and -1 (region 2 in Fig. 7), had on its own very little or no responsiveness to CCaMK/Cyclops mediated gene activation in *N. benthamiana* leaf cells, but such responsiveness was significantly boosted when

this region was combined with its 5' region containing *CYC-RE*<sub>*CBP1*</sub> (Fig. 5a). Interestingly, region 2, despite being devoid of a CCaMK/Cyclops response in *N. benthamiana* leaf cells, conferred gene expression in early nodule development, root vasculature and root tips in *L. japonicus* hairy roots infected by *M. loti* (Fig. S8). It remains to be clarified whether the expression in root vasculature and root tips is independent from rhizobia infection. Fourth, the region 5' of *EPRE*<sub>*CBP1*</sub> (between -2870 and -1327 bp, region 1 in Fig. 7) significantly enhances gene activation mediated by CCaMK/Cyclops in *N. benthamiana* leaf cells. Interestingly, the inclusion of this region in *N. benthamiana* transient assays resulted in much larger variation between different leaf discs and unusually strong inter-experimental variation. We interpret this variation as a sensitivity of the underlying regulatory machinery to subtle diurnal, developmental or environmental differences of the leaf tissue that are not observed in other promoter fusions. Deletion of this region did not result in loss of reporter expression in nodules, rather seemed to affect the expression strength of the reporter gene (Fig. 5b). Hence, we focussed only on the reporter gene expression pattern in the roots and did not further investigate a possible quantitative contribution of the -2780 and -1327 bp region.

In summary, we propose a model in which the *CBP1* promoter contains at least four distinct regulatory regions that contribute to the expression strength or the tissue specificity or the stimulus specificity of the *CBP1* expression.

### The T90 *white* mutant phenotype is caused by cytosine methylation of the T90 promoter

The initial forward genetic approach to screen an EMS-mutagenized T90 population led to the identification of the T90 *white* mutants (Fig. 2). Based on an analysis using cytosine methylation-sensitive restriction enzymes, we detected hypermethylation specifically in the T90 *white* mutants within *CYC-RE*<sub>*CBP1*</sub> (Fig. 4), which is capable on its own, to drive gene expression during AM and RNS (Fig. 6b). Cytosine methylation is a well-studied phenomenon and frequently associated with heterochromatin-based gene inactivation (Iwasaki & Paszkowski, 2014). The element's ability to achieve gene expression during both symbioses and its hypermethylation in the T90 *white* mutants are in line with the T90 and T90 *white* phenotype. However, hypermethylation is typically not restricted to single bases but generally affects longer DNA stretches that undergo heterochromatin formation. Indeed, we have obtained preliminary evidence for additional methylated cytosines within the 113 bp element depicted in Fig. 4 (data not shown). It is therefore likely that the T90 *white* mutants suffered from a broader hypermethylation within the T90 promoter and that the silencing of T90 cannot be attributed solely to the single cytosine methylation within *CYC-RE*<sub>*CBP1*</sub>. Independent of the extend of the hypermethylation in T90 *white* mutants, our observation revealed that Cyclops activity can be severely impeded by DNA methylation of its target promoters. As DNA methylation is overall dynamically altered during nodulation (Satgé, *et al.*, 2016), studying the methylation status of Cyclops target promoters may

reveal another layer of transcriptional regulation during symbiotic development.

### The role of CBP1 in symbiosis remains to be clarified

The CBP1 protein carries a predicted C-terminal calmodulin domain consisting of a double pair of EF hand calcium-binding motifs, and evidence for calcium-binding by CBP1 has been obtained (Tuck, 2006). Although reverse genetic evidence is still lacking, the common *CBP1* gene activation in both symbioses raises the possibility that CBP1 plays a role in calcium homeostasis or signalling in both types of endosymbiosis. Given the conserved function of the CaM domain to interact with calcium ions ( $\text{Ca}^{2+}$ ), other calcium-binding proteins (e.g. those that identified in Liao *et al.*, 2017) could function redundantly with CBP1 during symbiosis. Alternatively, it is possible that the residual expression of *CBP1* conferred by the 928 bp regulatory region 3' of the T-DNA insertion site in T90 (region 2 in Fig. 6) is sufficient for endosymbiosis or that the impact of the reduced expression levels could not be detected by phenotyping the number of nodules and shoot dry weight of plants (Fig. S4). Interestingly, the N-terminus of CBP1 is predicted to contain a signal peptide of 29 amino acid residue. This predicted signal peptide is highly similar to that of the Calmodulin-like protein 4 and 5 from *Arabidopsis thaliana* which are targeted to the endomembrane system of vesicular structures between Golgi and the endosomal system by their N-terminal anchor sequence (Ruge *et al.*, 2016). Understanding knowledge about the subcellular localization of CBP1 in terms of tissue type and subcellular space during RNS and AM symbiosis may help to further understand its function.

### Common and specific gene activation in AM and RNS mediated by *CYC-REs*

For most genes that are activated in both RNS and AM, the *cis*-elements responsible for this common induction are not yet known. Only one other element, an AT-rich motif identified in the promoter of *Medicago truncatula ENOD11* gene, was reported important for high-level gene expression during both RNS and AM (Boisson-Dernier *et al.*, 2005). *ENOD11* is one of the earliest marker genes induced by rhizobia as well as an AM fungus (Chabaud *et al.*, 2002; Journet *et al.*, 2001). The discovery of *CYC-RE<sub>CBP1</sub>* supported a possible scenario that at least a subset of the genes induced during both RNS and AM development could be regulated by the CCaMK/Cyclops complex. However, the common expression mediated by *CYC-RE<sub>CBP1</sub>* appears to be rather an exception than the rule: three *CYC-REs* identified earlier originate from the promoters of two RNS-induced genes, *NIN* and *ERN1* (hereafter called *CYC-RE<sub>NIN</sub>* and *CYC-RE<sub>ERN1</sub>*, respectively; Singh *et al.*, 2014; Cerri *et al.*, 2017) and an AM-induced gene, *RAM1* (hereafter called *CYC-RE<sub>RAM1</sub>*; Pimprikar *et al.*, 2016). The core of *CYC-RE<sub>CBP1</sub>* shares a high sequence similarity with *CYC-RE<sub>RAM1</sub>* and to a lesser extent with *CYC-RE<sub>NIN</sub>* and *CYC-RE<sub>ERN1</sub>*. The diversity observed in the *CYC-RE* sequences in terms of nucleotide composition, length, GC content and palindromic composition may indicate a direct

connection between *CYC-RE* sequence and the differential and potentially specific expression pattern governed by them in terms of symbiotic context or tissue type. Whether this is achieved by *CYC-REs* on their own or by collaboration with additional *cis*-elements and DNA-binding transcription factors, such as the identified interaction partners (Jin *et al.*, 2016; Pimprikar *et al.*, 2016) remains to be determined.





### Acknowledgements

The authors thank Judith K. Webb for the generation and initial characterisation of the transgenic line T90 and David Chiasson for providing a plasmid containing the *DoGUS* gene that is adapted for the Golden Gate cloning system. E. Jensen (née Tuck) thanks Aberystwyth University for a PhD scholarship. Work at The Sainsbury Laboratory was funded by the Gatsby Foundation. This work was supported by SFB924 'Molecular mechanisms regulating yield and yield stability in plants'. This project has received funding from the European Research Council (ERC) under the European Union's Seventh Framework Programme (FP7/2007–2013) under grant agreement no. 340904.

### Author contributions

MP performed mutagenesis of T90 seed to generate the T90 EMS mutant population (Fig. 2a) and EJ conducted screen B. SB performed screen A and investigated the T90 *white* phenotype. XG performed experiments and collected and analysed data (Figs 1, 2b–d, 3–5 and all Supporting Information figures). XG and MP drafted and finalized the manuscript. EJ contributed to manuscript editing.

### ORCID

Simone Bucerius  <https://orcid.org/0000-0002-6874-2081>  
Xiaoyun Gong  <https://orcid.org/0000-0003-1791-9382>  
Elaine Jensen  <https://orcid.org/0000-0003-2827-9819>  
Martin Parniske  <https://orcid.org/0000-0001-8561-747X>

### Data availability

Sequences of constructs and key plasmids necessary for reproducing the results are available at Addgene. Addgene deposit ID numbers can be found in Table S2.

### References

- Akamatsu A, Nagae M, Nishimura Y, Romero Montero D, Ninomiya S, Kojima M, Takebayashi Y, Sakakibara H, Kawaguchi M, Takeda N. 2020. Endogenous gibberellins affect root nodule symbiosis via transcriptional regulation of *NODULE INCEPTION* in *Lotus japonicus*. *The Plant Journal* 105: 1507–1520.
- Antolín-Llovera M, Petutsching EK, Ried MK, Lipka V, Nürnberger T, Robatzek S, Parniske M. 2014. Knowing your friends and foes - plant receptor-like kinases as initiators of symbiosis or defence. *New Phytologist* 204: 791–802.
- Banhara A, Ding Y, Kühner R, Zuccaro A, Parniske M. 2015. Colonization of root cells and plant growth promotion by *Piriformospora indica* occurs

- independently of plant common symbiosis genes. *Frontiers in Plant Science* 6. doi: 10.3389/fpls.2015.00667.
- Beringer JE. 1974. R factor transfer in *Rhizobium leguminosarum*. *Journal of General Microbiology* 84: 188–198.
- Binder A, Lambert J, Morbitzer R, Popp C, Ott T, Lahaye T, Parniske M. 2014. A modular plasmid assembly kit for multigene expression, gene silencing and silencing rescue in plants. *PLoS ONE* 9: e88218.
- Boisson-Dernier A, Andriankaja A, Chabaud M, Niebel A, Journet EP, Barker DG, de Carvalho-Niebel F. 2005. *MtENOD11* gene activation during rhizobial infection and mycorrhizal arbuscule development requires a common AT-rich-containing regulatory sequence. *Molecular Plant–Microbe Interactions* 18: 1269–1276.
- Bowler MW, Cliff MJ, Waltho JP, Blackburn GM. 2010. Why did Nature select phosphate for its dominant roles in biology? *New Journal of Chemistry* 34: 784–794.
- Breakspear A, Liu C, Roy S, Stacey N, Rogers C, Trick M, Morieri G, Mysore KS, Wen J, Oldroyd GE *et al.* 2014. The root hair “infectome” of *Medicago truncatula* uncovers changes in cell cycle genes and reveals a requirement for Auxin signaling in rhizobial infection. *Plant Cell* 26: 4680–4701.
- Cerri MR, Frances L, Laloum T, Auriac MC, Niebel A, Oldroyd GED, Baker DG, Fournier J, de Carvalho-Niebel F. 2012. *Medicago truncatula* ERN transcription factors: regulatory interplay with NSP1/NSP2 GRAS factors and expression dynamics throughout rhizobial infection. *Plant Physiology* 160: 2155–2172.
- Cerri MR, Wang Q, Stolz P, Folgmann J, Frances L, Katzer K, Li X, Heckmann AB, Wang TL, Downie JA *et al.* 2017. The ERN1 transcription factor gene is a target of the CCaMK/CYCLOPS complex and controls rhizobial infection in *Lotus japonicus*. *New Phytologist* 215: 323–337.
- Chabaud M, Venard C, Defaux-Petras A, Bécard G, Barker DG. 2002. Targeted inoculation of *Medicago truncatula* *in vitro* root cultures reveals *MtENOD11* expression during early stages of infection by arbuscular mycorrhizal fungi. *New Phytologist* 156: 265–273.
- Charpentier M, Bredemeier R, Wanner G, Takeda N, Schleiff E, Parniske M. 2008. *Lotus japonicus* Castor and Pollux are ion channels essential for perinuclear calcium spiking in legume root endosymbiosis. *Plant Cell* 20: 3467–3479.
- Deguchi Y, Banba M, Shimoda Y, Chechetka SA, Suzuri R, Okusako Y, Ooki Y, Toyokura K, Suzuki A, Uchiyama T *et al.* 2007. Transcriptome profiling of *Lotus japonicus* roots during arbuscular mycorrhiza development and comparison with that of nodulation. *DNA Research* 14: 117–133.
- Demina IV, Persson T, Santos P, Plaszczyca M, Pawlowski K. 2013. Comparison of the nodule vs. root transcriptome of the actinorhizal plant *Datisca glomerata*: actinorhizal nodules contain a specific class of defensins. *PLoS ONE* 8: e72442.
- Endre G, Kereszt A, Kevei Z, Mihacea S, Kaló P, Kiss GB. 2002. A receptor kinase gene regulating symbiotic nodule development. *Nature* 417: 962–966.
- Feng F, Sun J, Radhakrishnan GV, Lee T, Bozsóki Z, Fort S, Gavrin A, Gysel K, Thygesen MB, Andersen KR *et al.* 2019. A combination of chitoooligosaccharide and lipochitoooligosaccharide recognition promotes arbuscular mycorrhizal associations in *Medicago truncatula*. *Nature Communications* 10: 5047.
- Fowler D, Coyle M, Skiba U, Sutton MA, Cape JN, Reis S, Sheppard LJ, Jenkins A, Grizzetti B, Galloway JN *et al.* 2013. The global nitrogen cycle in the twenty-first century. *Philosophical Transactions of the Royal Society B: Biological Sciences* 368. doi: 10.1098/rstb.2013.0164.
- Gobbato E, Marsh J, Vernié T, Wang E, Maillat F, Kim J, Miller J, Sun J, Bano S, Ratet P *et al.* 2012. A GRAS-type transcription factor with a specific function in mycorrhizal signaling. *Current Biology* 22: 2236–2241.
- Gossmann JA. 2011. *Multiple molecular components contribute to genotype specific compatibility of the root nodule symbiosis*. PhD thesis, University of Munich, Munich, Germany.
- Gossmann JA, Markmann K, Brachmann A, Rose LE, Parniske M. 2012. Polymorphic infection and organogenesis patterns induced by a *Rhizobium leguminosarum* isolate from *Lotus* root nodules are determined by the host genotype. *New Phytologist* 196: 561–573.
- Groth M, Takeda N, Perry J, Uchida H, Dräxl S, Brachmann A, Sato S, Tabata S, Kawaguchi M, Wang TL *et al.* 2010. *NENA*, a *Lotus japonicus* homolog of *Sec13*, is required for rhizodermal infection by arbuscular mycorrhiza fungi and rhizobia but dispensable for cortical endosymbiotic development. *Plant Cell* 22: 2509–2526.
- Gutjahr C, Sawers RJH, Marti G, Andrés-Hernández L, Yang S-Y, Casieri L, Angliker H, Oakeley EJ, Wolfender J-L, Abreu-Goodger C *et al.* 2015. Transcriptome diversity among rice root types during asymbiosis and interaction with arbuscular mycorrhizal fungi. *Proceedings of the National Academy of Sciences, USA* 112: 6754–6759.
- Handberg K, Stougaard J. 1992. *Lotus japonicus*, an autogamous, diploid legume species for classical and molecular genetics. *The Plant Journal* 2: 487–496.
- Hoagland DR, Arnon DI. 1938. *The water-culture method for growing plants without soil*. University of California, Berkeley, CA, USA. [Revised by Arnon 1950].
- Hogekamp C, Arndt D, Pereira PA, Becker JD, Hohnjec N, Kuster H. 2011. Laser microdissection unravels cell-type-specific transcription in arbuscular mycorrhizal roots, including CAAT-box transcription factor gene expression correlating with fungal contact and spread. *Plant Physiology* 157: 2023–2043.
- Hohnjec N, Vieweg ME, Pühler A, Becker A, Küster H. 2005. Overlaps in the transcriptional profiles of *Medicago truncatula* roots inoculated with two different Glomus fungi provide insights into the genetic program activated during arbuscular mycorrhiza. *Plant Physiology* 137: 1283–1301.
- Ivanov S, Fedorova EE, Limpens E, de Mita S, Genre A, Bonfante P, Bisseling T. 2012. Rhizobium-legume symbiosis shares an exocytotic pathway required for arbuscule formation. *Proceedings of the National Academy of Sciences, USA* 109: 8316–8321.
- Iwasaki M, Paszkowski J. 2014. Epigenetic memory in plants. *EMBO Journal* 33: 1987–1998.
- Jefferson RA. 1987. Assaying chimeric genes in plants: the GUS gene fusion system. *Plant Molecular Biology Reporter* 5: 387–405.
- Jefferson RA, Kavanagh TA, Bevan MW. 1987. GUS fusions: beta-glucuronidase as a sensitive and versatile gene fusion marker in higher plants. *EMBO Journal* 6: 3901–3907.
- Jin Y, Liu H, Luo D, Yu N, Dong W, Wang C, Zhang X, Dai H, Yang J, Wang E. 2016. DELLA proteins are common components of symbiotic rhizobial and mycorrhizal signalling pathways. *Nature Communication* 7: 12433.
- Journet EP, El-Gachtouli N, Vernoud V, de Billy F, Pichon M, Dedieu A, Arnould C, Morandi D, Barker DG, Gianinazzi-Pearson V. 2001. *Medicago truncatula ENOD11*: a novel RPRP-encoding early nodulin gene expressed during mycorrhization in arbuscule-containing cells. *Molecular Plant–Microbe Interactions* 14: 737–748.
- Kim S, Zeng W, Bernard S, Liao J, Venkateshwaran M, Ane JM, Jiang Y. 2019. Ca<sup>2+</sup>-regulated Ca<sup>2+</sup> channels with an RCK gating ring control plant symbiotic associations. *Nature Communications* 10: 3703.
- Kistner C, Winzer T, Pitzschke A, Mulder L, Sato S, Kaneko T, Tabata S, Sandal N, Stougaard J, Webb KJ *et al.* 2005. Seven *Lotus japonicus* genes required for transcriptional reprogramming of the root during fungal and bacterial symbiosis. *Plant Cell* 17: 2217–2229.
- Kumar A, Cousins DR, Liu CW, Xu P, Murray JD. 2020. *Nodule inception* is not required for arbuscular mycorrhizal colonization of *Medicago truncatula*. *Plants* 9: 71.
- Lévy J, Bres C, Geurts R, Chalhoub B, Kulikova O, Duc G, Journet EP, Ané JM, Lauber E, Bisseling T *et al.* 2004. A putative Ca<sup>2+</sup> and calmodulin-dependent protein kinase required for bacterial and fungal symbioses. *Science* 303: 1361–1364.
- Liao J, Deng J, Qin Z, Tang J, Shu M, Ding C, Liu J, Hu C, Yuan M, Huang Y *et al.* 2017. Genome-wide identification and analyses of calmodulins and calmodulin-like proteins in *Lotus japonicus*. *Frontiers in Plant Science* 8: 482.
- Liu J, Blaylock LA, Endre G, Cho J, Town CD, VandenBosch KA, Harrison MJ. 2003. Transcript profiling coupled with spatial expression analyses reveals genes involved in distinct developmental stages of an arbuscular mycorrhizal symbiosis. *Plant Cell* 15: 2106–2123.
- Liu J, Rutten L, Limpens E, van der Molen T, van Velzen R, Chen R, Chen Y, Geurts R, Kohlen W, Kulikova O *et al.* 2019. A remote *cis*-regulatory region is required for *NIN* expression in the pericycle to initiate nodule primordium formation in *Medicago truncatula*. *Plant Cell* 31: 68–83.
- Lueders T, Manefeld M, Friedrich MW. 2004. Enhanced sensitivity of DNA- and rRNA-based stable isotope probing by fractionation and quantitative

- analysis of isopycnic centrifugation gradients. *Environmental Microbiology* 6: 73–78.
- Maekawa T, Kusakabe M, Shimoda Y, Sato S, Tabata S, Murooka Y, Hayashi M. 2008. Polyubiquitin promoter-based binary vectors for overexpression and gene silencing in *Lotus japonicus*. *Molecular Plant–Microbe Interactions* 21: 375–382.
- Maillet F, Poinso V, André O, Puech-Pagès V, Haouy A, Gueunier M, Cromer L, Giraudet D, Formey D, Niebel A *et al.* 2011. Fungal lipochitooligosaccharide symbiotic signals in arbuscular mycorrhiza. *Nature* 469: 58–64.
- Manthey K, Krajinski F, Hohnjec N, Firnhaber C, Pühler A, Perlick AM, Küster H. 2004. Transcriptome profiling in root nodules and arbuscular mycorrhiza identifies a collection of novel genes induced during *Medicago truncatula* root endosymbiosis. *Molecular Plant–Microbe Interactions* 17: 1063–1077.
- Márquez AJ. 2005. *Lotus japonicus handbook*. Dordrecht, the Netherlands: Springer.
- Medvedeva YA, Khamis AM, Kulakovskiy IV, Ba-Alawi W, Bhuyan MSI, Kawaji H, Lassmann T, Harbers M, Forrest ARR, Bajic VB. 2014. Effects of cytosine methylation on transcription factor binding sites. *BMC Genomics* 15: 119.
- Mendiburu F. 2018. Package 'AGRICOLAE'. [WWW document] URL <https://tarwi.lamolina.edu.pe/~fmendiburu/> [accessed 9 August 2021].
- Miller JB, Pratap A, Miyahara A, Zhou L, Bornemann S, Morris RJ, Oldroyd GED. 2013. Calcium/calmodulin-dependent protein kinase is negatively and positively regulated by calcium, providing a mechanism for decoding calcium responses during symbiosis signaling. *Plant Cell* 25: 5053–5066.
- Murray JD, Muni RRD, Torres-Jerez I, Tang Y, Allen S, Andriankaja M, Li G, Laxmi A, Cheng X, Wen J *et al.* 2011. *Vapyrin*, a gene essential for intracellular progression of arbuscular mycorrhizal symbiosis, is also essential for infection by rhizobia in the nodule symbiosis of *Medicago truncatula*. *The Plant Journal* 65: 244–252.
- Nanjareddy K, Arthikala MK, Gómez BM, Blanco L, Lara M. 2017. Differentially expressed genes in mycorrhizal and nodulated roots of common bean are associated with defense, cell wall architecture, N metabolism, and P metabolism. *PLoS ONE* 12: e0182328.
- Oldroyd GE. 2013. Speak, friend, and enter: signalling systems that promote beneficial symbiotic associations in plants. *Nature Reviews Microbiology* 11: 252–263.
- Perry JA, Brachmann A, Welham TJ, Binder A, Charpentier M, Groth M, Haage K, Markmann K, Wang TL, Parniske M. 2009. TILLING in *Lotus japonicus* identified large allelic series for symbiosis genes and revealed a bias in functionally defective ethyl methanesulfonate alleles toward glycine replacements. *Plant Physiology* 151: 1281–1291.
- Perry JA, Wang TL, Welham TJ, Gardner S, Pike JM, Yoshida S, Parniske M. 2003. A TILLING reverse genetics tool and a web-accessible collection of mutants of the legume *Lotus japonicus*. *Plant Physiology* 131: 866–871.
- Pimprikar P, Carbonnel S, Paries M, Katzer K, Klingl V, Bohmer M, Karl L, Floss D, Harrison M, Parniske M *et al.* 2016. A CCaMK-CYCLOPS-DELLA complex activates transcription of *RAM1* to regulate arbuscule branching. *Current Biology* 26: 987–998.
- Pimprikar P, Gutjahr C. 2018. Transcriptional regulation of arbuscular mycorrhiza development. *Plant and Cell Physiology* 59: 673–690.
- Radutoiu S, Madsen LH, Madsen EB, Felle HH, Umehara Y, Grønlund M, Sato S, Nakamura Y, Tabata S, Sandal N *et al.* 2003. Plant recognition of symbiotic bacteria requires two LysM receptor-like kinases. *Nature* 425: 585–592.
- Ried MK, Antolín-Llovera M, Parniske M. 2014. Spontaneous symbiotic reprogramming of plant roots triggered by receptor-like kinases. *eLife* 3: e03891.
- Roux B, Rodde N, Jardinaud M-F, Timmers T, Sauviac L, Cottret L, Carrère S, Sallet E, Courcelle E, Moreau S *et al.* 2014. An integrated analysis of plant and bacterial gene expression in symbiotic root nodules using laser-capture microdissection coupled to RNA sequencing. *The Plant Journal* 77: 817–837.
- Roy S, Breakspear A, Cousins D, Torres-Jerez I, Jackson KJ, Kumar A, Su Y, Krom N, Liu C-W, Udvardi M *et al.* 2021. Three common symbiotic ABC-B transporters in *Medicago truncatula* are regulated by a NIN-independent branch of the symbiosis signalling pathway. *Molecular Plant–Microbe Interactions* 34: 939–951.
- Ruge H, Flosdorff S, Ebersberger I, Chigri F, Vothknecht C. 2016. The calmodulin-like proteins AtCML4 and AtCML5 are single-pass membrane proteins targeted to the endomembrane system by an N-terminal signal anchor sequence. *Journal of Experimental Botany* 67: 3985–3996.
- Sakamoto K, Ogiwara N, Kaji T, Sugimoto Y, Ueno M, Sonoda M, Matsui A, Ishida J, Tanaka M, Totoki Y *et al.* 2019. Transcriptome analysis of soybean (*Glycine max*) root genes differentially expressed in rhizobial, arbuscular mycorrhizal, and dual symbiosis. *Journal of Plant Research* 132: 541–568.
- Satgé C, Moreau S, Sallet E, Lefort G, Auriac M-C, Remblière C, Cottret L, Gallardo K, Noïrot C, Jardinaud M-F *et al.* 2016. Reprogramming of DNA methylation is critical for nodule development in *Medicago truncatula*. *Nature Plants* 2: 16166.
- Schauser L, Roussis A, Stiller J, Stougaard J. 1999. A plant regulator controlling development of symbiotic root nodules. *Nature* 402: 191–195.
- Schultze M, Kondorosi A. 1998. Regulation of symbiotic root nodule development. *Annual Review of Genetics* 32: 33–57.
- Sieberer BJ, Chabaud M, Timmers AC, Monin A, Fournier J, Barker DG. 2009. A nuclear-targetedameleon demonstrates intranuclear Ca<sup>2+</sup> spiking in *Medicago truncatula* root hairs in response to rhizobial nodulation factors. *Plant Physiology* 151: 1197–1206.
- Singh S, Katzer K, Lambert J, Cerri M, Parniske M. 2014. CYCLOPS, a DNA-binding transcriptional activator, orchestrates symbiotic root nodule development. *Cell Host and Microbe* 15: 139–152.
- Stracke S, Kistner C, Yoshida S, Mulder L, Sato S, Kaneko T, Tabata S, Sandal N, Stougaard J, Szczygłowski K *et al.* 2002. A plant receptor-like kinase required for both bacterial and fungal symbiosis. *Nature* 417: 959–962.
- Szczygłowski K, Shaw RS, Wopereis J, Copeland S, Hamburger D, Kasiborski B, Dazzo FB, de Bruijn FJ. 1998. Nodule organogenesis and symbiotic mutants of the model legume *Lotus japonicus*. *Molecular Plant–microbe Interactions* 11: 684–697.
- Takeda N, Kistner C, Kosuta S, Winzer T, Pitzschke A, Groth M, Sato S, Kaneko T, Tabata S, Parniske M. 2007. Proteases in plant root symbiosis. *Phytochemistry* 68: 111–121.
- Takeda N, Maekawa T, Hayashi M. 2012. Nuclear-localized and deregulated calcium- and calmodulin-dependent protein kinase activates rhizobial and mycorrhizal responses in *Lotus japonicus*. *Plant Cell* 24: 810–822.
- Takeda N, Sato S, Asamizu E, Tabata S, Parniske M. 2009. Apoplastic plant subtilases support arbuscular mycorrhiza development in *Lotus japonicus*. *Plant Journal* 58: 766–777.
- Tirichine L, Imaizumi-Anraku H, Yoshida S, Murakami Y, Madsen LH, Miwa H, Nakagawa T, Sandal N, Albrektzen AS, Kawaguchi M *et al.* 2006. Deregulation of a Ca<sup>2+</sup>/calmodulin-dependent kinase leads to spontaneous nodule development. *Nature* 441: 1153–1156.
- Topping JF, Wei W, Lindsey K. 1991. Functional tagging of regulatory elements in the plant genome. *Development* 112: 1009–1019.
- Tomas A, Parizot B, Diagne N, Champion A, Hocher V, Cissoko M, Crabos A, Prodjinoto H, Lahouze B, Bogusz D *et al.* 2012. Heart of endosymbioses: transcriptomics reveals a conserved genetic program among arbuscular mycorrhizal, actinorhizal and legume-rhizobial symbioses. *PLoS ONE* 7: e44742.
- Tuck E. 2006. *Molecular and genetic analysis of a symbiosis-specific locus of the Lotus japonicus genome and its potential as a tool for dissecting the symbiotic signal transduction pathway*. PhD thesis, University of Aberystwyth, Aberystwyth, Wales, UK. [WWW document] URL [https://pure.aber.ac.uk/portal/files/49036338/Jensen\\_Elaine.pdf](https://pure.aber.ac.uk/portal/files/49036338/Jensen_Elaine.pdf) [accessed 9 November 2021].
- Voinnet O, Rivas S, Mestre P, Baulcombe D. 2003. An enhanced transient expression system in plants based on suppression of gene silencing by the p19 protein of tomato bushy stunt virus. *The Plant Journal* 33: 949–956.
- Webb KJ, Skøt L, Nicholson MN, Jørgensen B, Mizen S. 2000. *Mesorhizobium loti* increases root-specific expression of a calcium-binding protein homologue identified by promoter tagging in *Lotus japonicus*. *Molecular Plant–microbe Interactions* 13: 606–616.
- Wegel E, Schauser L, Sandal N, Stougaard J, Parniske M. 1998. Mycorrhizal mutants of *Lotus japonicus* define genetically independent steps during symbiotic infection. *Molecular Plant–microbe Interactions* 11: 933–936.

- Wickham H, Stryjewski L. 2011. *40 years of boxplots*. [WWW document] URL <https://vita.had.co.nz/papers/boxplots.pdf> [accessed 9 August 2021].
- Yang L, Chen Z, Stout ES, Delerue F, Ittner LM, Wilkins MR, Quinlan KGR, Crossley M. 2020. Methylation of a CGATA element inhibits binding and regulation by GATA-1. *Nature Communications* 11: 2560.
- Yano K, Yoshida S, Müller J, Singh S, Banba M, Vickers K, Markmann K, White C, Schuller B, Sato S *et al.* 2008. CYCLOPS, a mediator of symbiotic intracellular accommodation. *Proceedings of the National Academy of Sciences, USA* 105: 20540–20545.
- Zhang C, He J, Dai H, Wang G, Zhang X, Wang C, Shi J, Chen X, Wang D, Wang E. 2021. Discriminating symbiosis and immunity signals by receptor competition in rice. *Proceedings of the National Academy of Sciences, USA* 118: e2023738118.

## Supporting Information

Additional Supporting Information may be found online in the Supporting Information section at the end of the article.

**Fig. S1** T90 roots or nodules displayed GUS activity at 3, 7 or 21 dpi *Mesorhizobium loti* DsRed.

**Fig. S2** T90 *white* mutants lost symbiosis-induced *GUS* expression in the roots but retained symbiosis competence.

**Fig. S3** Ectopic expression of autoactive CCaMK<sup>T265D</sup> in T90 hairy roots induced weak *GUS* expression in root epidermis.

**Fig. S4** Spatio-temporal *GUS* expression in *Lotus japonicus* hairy roots transformed with promoter : *GUS* fusions during nodulation.

**Fig. S5** Differential cytosine methylation within the *CYC-RE<sub>CBP1</sub>* between T90 *white* mutants, T90 and *Lotus japonicus* Gifu.

**Fig. S6** A *cis*-element in the *CBP1* promoter is necessary and sufficient for CCaMK<sup>1–314</sup>/Cyclops-mediated transactivation.

**Fig. S7** *GUS* expression in *Lotus japonicus* hairy roots transformed with *T90<sub>pro</sub>-GUS* at an early stage of infection by AM fungus *Rhizophagus irregularis*.

**Fig. S8** *CBP1* promoter-driven reporter gene expression during nodulation in *Lotus japonicus* roots.

**Methods S1** Plant, bacterial and fungal material.

**Methods S2** Plant growth condition and phenotypic analysis.

**Methods S3** Staining method for arbuscular mycorrhizal fungi visualization.

**Table S1** Seed bags used in this study.

**Table S2** Constructs and primers used in this study.

**Table S3** Predicted transcription factor binding site in *EPRE<sub>CBP1</sub>*.

Please note: Wiley Blackwell are not responsible for the content or functionality of any Supporting Information supplied by the authors. Any queries (other than missing material) should be directed to the *New Phytologist* Central Office.